Clim Dyn
DOI 10.1007/s00382-011-1026-0

Conceptual understanding of climate change with a globally resolved energy balance model

Dietmar Dommenget · Janine Flöter

Received: 28 April 2010 / Accepted: 7 February 2011

Abstract The future climate change projections are essentially based on coupled general circulation model (CGCM) simulations, which give a distinct global warming pattern with arctic winter amplification, an equilibrium land-sea warming contrast and an inter-hemispheric warming gradient. While these simulations are the most important tool of the Intergovernmental Panel on Climate Change (IPCC) predictions, the conceptual understanding of these predicted structures of climate change and the causes of their uncertainties is very difficult to reach if only based on these highly complex CGCM simulations. In the study presented here we will introduce a very simple, globally resolved energy balance (GREB) model, which is capable of simulating the main characteristics of global warming. The model shall give a bridge between the strongly simplified energy balance models and the fully coupled 4-dimensional complex CGCMs. It provides a fast tool for the conceptual understanding and development of hypotheses for climate change studies, which shall build a basis or starting point for more detailed studies of observations and CGCM simulations. It is based on the surface energy balance by very simple representations of solar and thermal radiation, the atmospheric hydrological cycle, sensible turbulent heat flux, transport by the mean atmospheric circulation and heat exchange with the deeper ocean. Despite some limitations in the representations of the basic processes, the models climate sensitivity and the spatial structure of the warming pattern are within the uncertainties of the IPCC models simulations. It is capable of simulating aspects of the arctic winter amplification, the equilibrium land-sea warming contrast and the inter-hemispheric warming gradient with good agreement to the IPCC models in amplitude and structure. The results give some insight into the understanding of the land-sea contrast and the polar amplification. The GREB model suggests that the regional inhomogeneous distribution of atmospheric water vapor and the non-linear sensitivity of the downward thermal radiation to changes in the atmospheric water vapor concentration partly cause the land-sea contrast and may also contribute to the polar amplification. The combination of these characteristics causes, in general, dry and cold regions to warm more than other regions.

Keywords Climate dynamics · Climate change · Climate models · Simple climate model · Climate feedback · Climate sensitivity · Energy balance model · Global warming

1 Introduction

The early estimates of climate change due to changes in the greenhouse gases started with simple energy balance considerations (e.g. Arrhenius 1896; Sellers 1969; Budyko 1972 or see North et al. 1981 for a review). With increasing computing power the climate models developed from simple energy balance models into fully coupled complex general circulation models (e.g. Manabe and Stouffer 1980 or Meehl et al. 2007a, b and references therein). The main aim in model development is to improve the

Electronic supplementary material The online version of this article (doi:10.1007/s00382-011-1026-0) contains supplementary material, which is available to authorized users.

D. Dommenget (✉)
School of Mathematical Sciences, Monash University, Melbourne, VIC 3800, Australia
e-mail: dietmar.dommenget@monash.edu

J. Flöter
Leibniz Institute for Marine Sciences, IFM-GEOMAR, Kiel, Germany

Published online: 18 March 2011

representation of the main physical processes and to include more processes that affect aspects of the climate system. The CGCMs are subsequently focusing on the best possible simulation of the climate system, but not necessarily on the best conceptual understanding of the phenomena of the climate and its variability or change. While the models became more realistic in simulating the climate mean state, they also become more complex. In present-day CGCMs it is far from trivial to understand even simple aspects of the climate system, because too many processes interact with each other in CGCM simulation.

Simplified models such as the earth system models of intermediate complexity (EMICs) are capable of simulating the large scale features of climate change (see Petoukhov et al. 2005 or references within). This raises the question, whether the main large-scale features of the global warming pattern, predicted by the IPCC model simulations, may indeed be simulated with a strongly simplified model, in which only the main processes are considered in strongly simplified representations. This study aims to present such a strongly simplified model. Although, the model introduced in this study will have some significant limitations in the representation of the main processes, this first version of the model already illustrates that the main large-scale features can indeed be understood by only a few simplified processes. The model shall be understood as a simple tool, which helps to conceptually understand aspects of the global warming response. It can help to develop hypotheses about the processes involved in aspects of climate change or climate variability, which must further be tested with observations or more complex and more realistic CGCM simulations. We will apply the simple model to several aspects of the large-scale climate change pattern.

The land-sea warming contrast, with stronger warming over land than over oceans, is probably one of the best known features of the observed and predicted global warming pattern. It has in the past been pointed out that this phenomenon is not just a transient effect due to different heat capacities over land and oceans, but is indeed an intrinsic feature of climate dynamics that persists even in the equilibrium $2 \times CO_2$ response (e.g. Manabe et al. 1991). However, only very recent studies focused on this phenomenon in more detail (Sutton et al. 2007; Joshi et al. 2008; Lambert and Chiang 2007). Joshi et al. (2008) suggest that the equilibrium land-sea warming contrast is caused by regional differences in the hydrological cycle. Over oceans water vapor is evaporated much more strongly than over land, causing stronger latent heat release into the troposphere. The additional warming in the atmosphere is than mixed globally by the atmospheric circulation causing the land to warm more strongly than the oceans. Dommenget (2009) argues, that additionally water vapor will be mixed globally by the atmospheric circulation, causing additional heating over land by radiative feedbacks and possibly additional latent heat release by condensation or precipitation. In the study presented here we will use the simple model to conceptually deconstruct the land-sea contrast to illustrate the feedbacks involved in this phenomenon.

The polar amplification is one of the most prominent features of the observed and predicted future global warming pattern (see Serreze and Francis 2006 for an overview). It is mostly argued to result from the sea ice cover/snow-albedo feedbacks (e.g. Budyko 1969; Sellers 1969; Manabe and Stouffer 1980; Serreze and Francis 2006; Meehl et al. 2007a, b), but other studies also find indications that the arctic amplification exists without the snow/ice-albedo feedback (e.g. Hall 2004; Alexeev et al. 2005; Cai 2006; Langen and Alexeev; 2007, Graversen and Wang 2009 or Lu and Cai 2010). The clear sky water vapor feedback is strongly increased in the polar regions due to the very low atmospheric concentrations of water vapor in the cold arctic winter (Curry et al. 1995) and Winton (2006) found that the long wave radiation response appears to be an important factor. Both results may indicate that water vapor feedbacks may be important in the arctic amplification as well. In the following study presented here, we will use the simple climate model to take a look on how the sea ice/snow-albedo, the water vapor feedbacks, and other processes in the climate system interact with each other to produce the polar amplification, which may contribute to the understanding of the arctic warming.

The paper is organized as follows: The following section describes the data and additional GCM simulation used. The main concept and details of the globally resolved energy balance (GREB) model introduced in this study are presented in Sect. 3, which is followed by a discussion of the GREB model's climate sensitivity in comparison with that of the IPCC-models. Section 4 presents a discussion of the conceptual deconstruction of the global warming pattern, the land-sea contrast and the polar amplification. The final section gives a summary and discussion of the main findings.

2 Data and additional ECHAM5 experiments

Most climatological values are taken from the NCEP reanalysis data from 1950 to 2008 (Kalnay et al. 1996), see Table 1. The cloud cover climatology is taken from the ISCCP project (Rossow and Schiffer 1991). The ocean mixed layer depth climatology is taken from Lorbacher et al. (2006). The gaps of the original Lorbacher et al. (2006) climatology are filled by a simple nearest neighbor interpolation and the seasonal evolution is smoothed by an annual and semiannual harmonics fit. Topographic data was taken from ECHAM5 atmosphere model (Roeckner et al. 2003). See Fig. 1 for the mean climatologies of the

Table 1 List of prognostic and important diagnostic variables and climatological boundary conditions used in the GREB model

Prognostic variables	Meaning	Comment
T_{surf}	Surface temperature	Reference climatology taken from the NCEP mean 2 m air temperature from 1950 to 2008
T_{atmos}	Temperature of the atmosphere	Roughly the Temperature of the lower troposphere above the boundary layer without adiabatic cooling; simulates the atmospheric circulation and the latent heat release
T_{ocean}	Temperature of the subsurface ocean	Temperature of the subsurface ocean of the upper 600 m; simulates the ocean heat uptake. The climatological mean is forced to be the min(T_{surf})
q_{air}	Humidity of the surface layer	Reference climatology taken from the NCEP mean from 1950 to 2008

Diagnostic variables	Meaning	Comment
$viwv_{atmos}$	Vertically integrated atmospheric water vapor	Proportional to q_{air}; used for the computation of the effective emissivity ε_{atmos} only
γ_{surf}	Heat capacity of surface layer	Fixed over land; climatological ocean mixed layer depth over ice free ocean; diagnostic for sea ice
α_{surf}	Surface albedo	Only a function of T_{surf}
α_{cloud}	Albedo of the atmosphere	Only a function of CLD $\alpha_{cloud} = 0.6\ CLD$
α_{total}	Total albedo	$\alpha_{total} = \alpha_{surf} + \alpha_{cloud} - \alpha_{surf}\,\alpha_{cloud}$
ε_{atmos}	Effective total emissivity	See Eqs. 4 and 5

Climatological boundary conditions	Meaning	Comment
CO_2	Atmospheric CO_2 mixing ratio	Depending on scenario
z_{topo}	Topographic height	Only over land; ocean depth is constant
$\vec{u}$	Atmospheric mean horizontal wind	Reference climatology taken from the NCEP 850 hPa level mean from 1950 to 2008
ϑ_{soil}	Surface wetness fraction	Reference climatology taken from the NCEP mean from 1950 to 2008
h_{mld}	Ocean mixed layer depth	Reference climatology taken from Lorbacher et al. (2006)
CLD	Total cloud cover	Climatology taken from the ISCCP project (Rossow and Schiffer 1991)

boundary conditions used for the GREB model. Glacier points are those that are higher than 300 m in Topographic and whose annual mean and maximum monthly mean temperature are below 5°C.

Additional experiments with the ECHAM5 atmosphere model in T31 resolution (Roeckner et al. 2003) coupled to a simple mixed layer ocean model (Dommenget and Latif 2008) are performed to estimate characteristics of the downward thermal radiation dependence in respect to atmospheric water vapor and cloud cover.

The IPCC model simulations are taken from the CMIP3 database (Meehl et al. 2007a, b). The IPCC-ensemble mean is taken from 24 model simulations of the IPCC A1B-scenario.

3 The globally resolved energy balance model (GREB)

The main idea of the simple globally resolved energy balance model is: (1) to reduce the complexity of the climate system; (2) to allow a stepwise deconstruction of the climate change response; (3) to avoid mean state climate biases and allow sensitivity studies with alterations in the climate mean state; (4) to have a simple conceptual model that is on the same or comparable horizontal grid resolution as the CGCM simulations and (5) to have a fast and easy to use tool for studies of the climate system response to external forcings.

The processes simulated with the GREB model are illustrated in Fig. 2. Each of these processes is represented with strongly simplified equations. The primary prognostic variable of the GREB model is the surface temperature, T_{surf}, which follows the tendency equation:

$$\gamma_{surf}\frac{dT_{surf}}{dt} = F_{solar} + F_{thermal} + F_{latent} + F_{sense} + F_{ocean} + F_{correct} \quad (1)$$

The tendencies of T_{surf} are forced by the incoming solar radiation, F_{solar}, the net thermal radiation, $F_{thermal}$, the

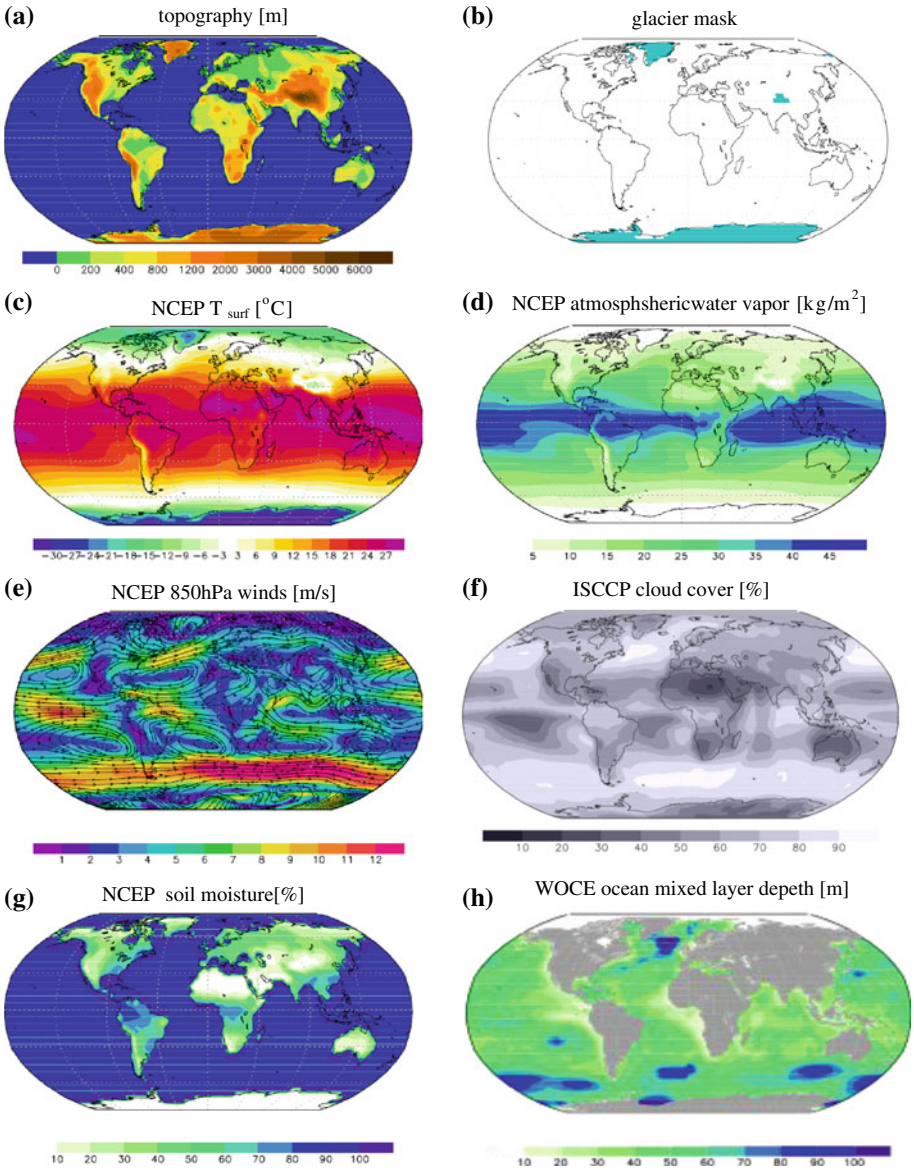

Fig. 1 GREB mean state climate boundary conditions: topography (**a**), glacier mask (**b**), T_{surf} (**c**), $VIWV_{atmos}$ (**d**), $\vec{u}$ (**e**), cloud cover (**f**), ϑ_{soil} (**g**), and h_{mld} (**h**)

cooling by latent heat from surface evaporation of water, F_{latent}, the turbulent heat exchange with the atmosphere, F_{sense}, and the heat exchange with the deeper subsurface ocean, F_{ocean}. Each of these forcing terms is related to one or more of the processes illustrated in Fig. 2. The flux correction term, $F_{correct}$, is an empirical correction of the tendencies of T_{surf} to correct for model errors. The surface heat capacity, γ_{surf}, is for ice free ocean points assumed to be the heat capacity of the ocean mixed layer, which follows the seasonal cycle of the mixed layer depth, h_{mld}, with regional differences (see Fig. 1h) and is that of a 2 m soil for land points. It varies for sea ice points as discussed further below. The processes are modeled as follows:

3.1 Solar radiation

The absorbed incoming solar radiation is given by

$$F_{solar} = (1 - \alpha_{clouds}) \cdot (1 - \alpha_{surf}) \cdot S_0 \cdot r(\lambda, t_{julian}) \qquad (2)$$

with the solar constant S_0, the 24 h mean fraction reaching a normal surface area on top of the atmosphere, r, as function of latitude, λ, and the Julian day of the calendar year, t_{julian} (Sellers 1965). A fraction of the incoming solar radiation is reflected by clouds, α_{clouds}, and by the surface, α_{surf}. The cloud albedo, α_{clouds}, is assumed to be proportional to the total cloud cover, which is given as a seasonal climatology (see Fig. 1f). For complete cloud cover $\alpha_{clouds} = 0.35$.

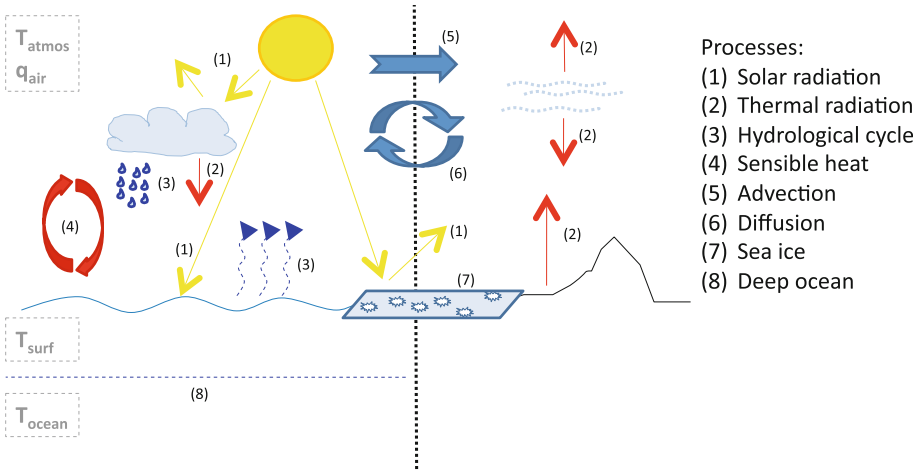

Fig. 2 A sketch of the physical processes considered in the GREB model

The surface albedo, α_{surf}, is assumed to be a linear function of T_{surf} within a temperature interval near the freezing point of water and constant outside this temperature interval, see Fig. 3a. Within the temperature interval, where α_{surf}, is a function of T_{surf}, the solar radiation represents a strong positive feedback. This temperature dependence shall reflect a simple parameterization of the surface albedo dependence on the snow/ice-cover over land and sea ice cover over oceans, which is similar to other simple model approaches (e.g. Sellers 1976; Ramanathan 1977). The large glaciers of Greenland and Antarctica, for instance, are kept with a constant albedo, assuming that they will not change, see Fig. 1b for the glacier mask.

Figure 3c, d illustrates where the snow-albedo feedback is active. During wintertime T_{surf} is within the temperature interval (−10°C, 0°C) only in a band around 40–50°N. The strength of the feedback is also altered by the incoming solar radiation and by the cloud cover. Since the solar radiation in high latitudes winter is very weak, the ice-albedo feedback is also weaker the further north it goes. In summertime the feedback is much weaker and mostly in the Arctic Sea.

We neglect any cloud feedbacks on the albedo in this formulation, due to the large uncertainty of the main feedback and its regional structure, although it may in principle be possible to include a simple feedback formulation in this model. Note also, that regional and seasonal variations in α_{surf} without snow/ice cover changes (e.g. vegetation) are also neglected.

3.2 Thermal radiation

The thermal radiation forcing to T_{surf} is due to the black body emission of the surface and due to the atmospheric downward thermal radiation, which depends on the

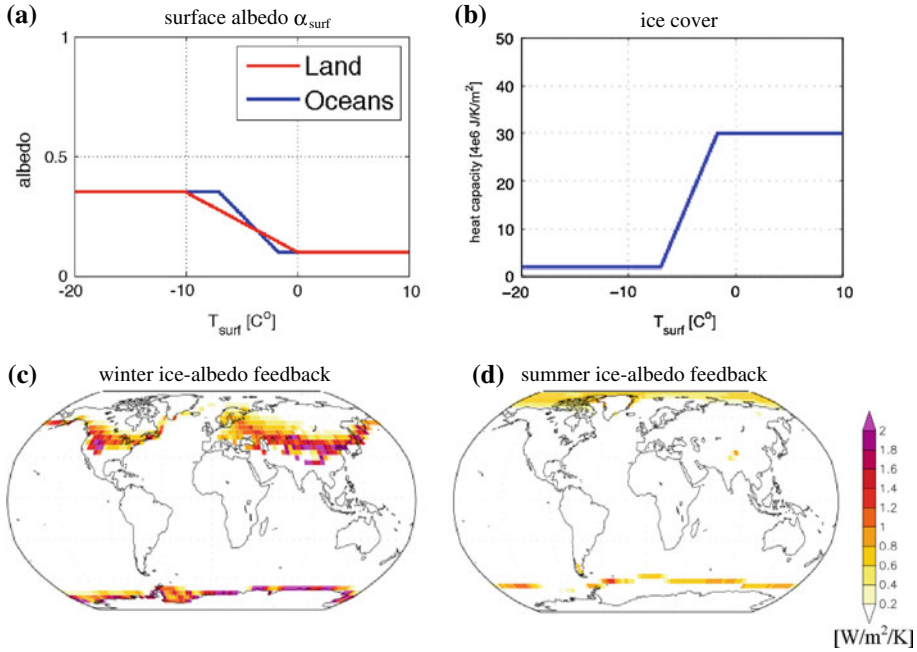

Fig. 3 **a** The parameterization of the surface albedo α_{surf}. **b** The surface layer heat capacity as function of T_{surf}. **c**, **d** The mean ice-albedo feedback for winter (JFM) and summer (JAS) in the GREB model

atmospheric temperature, T_{atmos}, the CO_2 concentration, the vertical integrated atmospheric water vapor concentration, $viwv_{atmos}$, and the cloud cover. It is the only way the greenhouse gas CO_2 influences the climate system, but it also represents the most fundamental negative feedback to increasing T_{surf} and the most important positive feedback due to atmospheric water vapor response. Simple climate models (e.g. Harvey and Schneider 1985; Weaver et al. 2001) use different approaches to simulate the long wave radiation, which mostly include some parameterizations of the surface outgoing and atmospheric downward radiation (e.g. Ramanathan 1977; Ramanathan et al. 1979; Fanning and Weaver 1996). We try to keep the model as simple as possible with the least number of parameters and base our thermal radiation model on the slab atmosphere greenhouse model (Bohren and Clothiaux 2006).

The net thermal radiation is due to a loss by outgoing thermal radiation and a gain by atmospheric thermal radiation:

$$F_{thermal} = -\sigma T_{surf}^4 + \varepsilon_{atmos}\sigma T_{atmos-rad}^4 \quad (3)$$

The atmosphere is radiating with the temperature $T_{atmos\text{-}rad}$ and an effective emissivity, ε_{atmos}. $T_{atmos\text{-}rad}$ will be defined in the context of the atmospheric temperature, T_{atmos}, in Sect. 3.4. The effective emissivity, ε_{atmos}, is depending on the CO_2 concentration, the vertical integrated atmospheric water vapor concentration, $viwv_{atmos}$, and the cloud cover. As a simple approximation of the dependency on CO_2 and $viwv_{atmos}$ we use a log-function approach as in Myhre et al. (1998). We also need to consider that the absorption and emission of thermal radiation at different spectral bands are overlapping for CO_2 and $viwv_{atmos}$ (e.g. Kiehl and Ramanathan 1982). This can be approximated by:

$$\begin{aligned}\varepsilon_0 = {} & pe_4 \cdot \log\left[pe_1 \cdot CO_2^{topo} + pe_2 \cdot viwv_{atmos} + pe_3\right] \\ & + pe_5 \cdot \log\left[pe_1 \cdot CO_2^{topo} + pe_3\right] \\ & + pe_6 \cdot \log\left[pe_2 \cdot viwv_{atmos} + pe_3\right] + pe_7 \end{aligned} \quad (4)$$

ε_0 is the emissivity without considering clouds first. CO_2^{topo} is the atmospheric concentration of CO_2 scaled by changes in surface pressure due to the topographic height, z_{topo}: $CO_2^{topo} = e^{-z_{topo}/z_{atmos}} \cdot CO_2$. The scaling height $z_{topo} =$ 8,400 m is a measure of the thickness of the atmosphere. The first term RHS (right hand side) in Eq. 4 is the emissivity due to CO_2, $viwv_{atmos}$ and some residual component, pe_3, in spectral bands where the components thermal emissivity overlaps. The second and third term RHS are the non-overlapping spectral bands CO_2 and $viwv_{atmos}$ terms (they still overlap with pe_3). The parameters pe_{4-6} give the relative importance of each absorption band, pe_{1-3} are the greenhouse gas species scaling concentration, which we assume to be the same for each absorption band to simplify the approximation. The log-function approach is a simple approximation to consider the saturation effective. Note that this ε-function can be <0 and >1, but in all simulations discussed in this study such values are not reached. It needs to be noted that the slab greenhouse is an approximation. If greenhouse gasses increase, a multi layer model would be better, which effectively means that ε_{atmos} can become larger than one (Bohren and Clothiaux 2006). If no greenhouse gasses exist ε_{atmos} should be zero. It is an extreme case (e.g. no CO_2, $VIWV$ and cloud cover), but should be considered.

Cloud cover is considered by:

$$\varepsilon_{atmos} = \frac{pe_8 - CLD}{pe_9} \cdot (\varepsilon_0 - pe_{10}) + pe_{10} \quad (5)$$

Thus cloud cover, CLD, scales the effective emissivity, ε_{atmos}, by shifting it up or down and by diluting the effects of the trace gasses. So in the presence of clouds emissivity is larger and the effect of trace gas concentrations is reduced. This also reduces the sensitivity to changes in trace gasses concentration. The parameters of the model are fitted to literature values constraining the effective emissivity as function of CO_2, $viwv_{atmos}$, and CLD with an iterative numerical fitting routine minimizing a cost-function (see Appendix 2 for details).

The main characteristics of the ε_{atmos} function are illustrated in Fig. 4. ε_{atmos} increases due to $viwv_{atmos}$ and CLD, while the CLD leads to stronger increases when $viwv_{atmos}$ is low (Fig. 4a). Further we can see that the spectral overlap of CO_2 with $viwv_{atmos}$ leads to a smaller sensitivity to CO_2 when $viwv_{atmos}$ is large (Fig. 4c). In summary we have a non-linear model for the emissivity as function of CO_2 concentration, $viwv_{atmos}$, and the cloud cover. This simplified approach of estimating the downward thermal radiation, neglects details of the vertical atmospheric structure (e.g. temperature, cloud thickness, trace gases). Changes or feedbacks in the vertical temperature and radiation structure are known as the lapse rate feedbacks (e.g. Ramanathan 1977 or Soden and Held 2006 and references therein).The approach chosen here represents a very strong simplification of the thermal radiation transfer within the atmosphere, which is simulated in CGCM by the vertical integral of long wave radiation transfer through the atmosphere, depending on the vertically resolved temperature, emissivity, density, cloudiness, atmospheric trace gas composition, etc. The simple model (Eqs. 4 and 5) is certainly not optimal and can not reproduce the full complexity of the atmospheric thermal radiation. In particular extreme cases, such as very low $viwv_{atmos}$ (<1 kg/m^2) or CO_2 (<50 ppm), for instance, are likely to be not well describe by this model. It further needs to be noted that this model is derived on the basis of the GCM models, whereas it should rather be based on observations. However, a global estimate of this

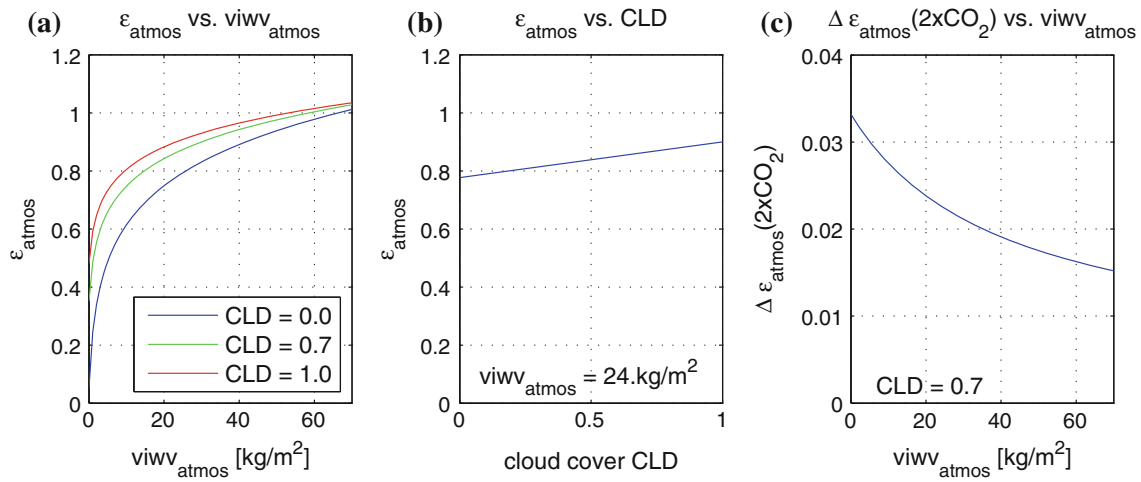

Fig. 4 **a** ε_{atmos} as function of $viwv_{atmos}$ for three different CLD following Eq. 5. **b** ε_{atmos} as function of CLD. **c** $\Delta\varepsilon_{atmos}$ $(2 \times CO_2)$ as function of $viwv_{atmos}$

relationship from observations is also uncertain due to limited observations. Further an adequate estimate of this parameterization would require a much more detailed discussion, which is beyond the scope of this paper.

However, for the first formulation of the GREB model we think the model estimate is sufficient, while further development of the model should include an observational based estimate. The thermal radiation feedbacks are most likely the largest uncertainties and systematic errors in the GREB model formulation, which will partly be discussed in the analysis of the model global warming response pattern.

3.3 Hydrological cycle

The response in $viwv_{atmos}$ and the latent heat release is central to climate change. We therefore have to simulate the response of the hydrological cycle, which includes the evaporation of water vapor at the surface, the condensation of water in the atmosphere and the associated take-up and releases of latent heat at the surface and in the atmosphere, respectively. The saturation surface air layer specific humidity, q_{sat}, is given by

$$q_{sat} = e^{-z_{topo}/z_{atmos}} \cdot 3.75 \cdot 10^{-3} \cdot e^{\left(17.08085\frac{T_{surf}-273.15}{T_{surf}-38.975}\right)} \quad (6)$$

which is taken from the textbook from James (1994) and extended to consider changes in surface pressure due to the topographic height, z_{topo}. The latent heat release to the surface layer associated with evaporation is given by an extended Bulk formula (Peixoto and Oort 1992a, 1992b):

$$F_{latent} = L \cdot \rho_{air} \cdot C_w \cdot |\vec{u}_*| \cdot \vartheta_{soil} \cdot (q_{air} - q_{sat}) \quad (7)$$

The Bulk formula depends on the difference between q_{sat} and the actual surface air layer humidity, q_{air}, the wind speed, $|\vec{u}_*|$ the constant parameters of the latent heat of evaporation and condensation of water, L, the density of air, ρ_{air}, and the transfer coefficient, C_w. The wind speed, $|\vec{u}_*|$ is assumed to be the seasonally varying mean winds of the NCEP reanalysis 850 hPa geopotential height winds, $\vec{u}$ (see Fig. 1e for the annual mean values) plus a globally constant turbulent part of 3 m/s over oceans and 2 m/s over land. The Bulk formula is extended by a surface wetness fraction, ϑ_{soil}, to simulate evaporation over land, where the surface is not always wet. ϑ_{soil} is assumed to be a climatological boundary condition in the GREB model, which however varies with the seasonal cycle, see Fig. 1g for the annual mean values.

The atmospheric integrated water vapor, $viwv_{atmos}$, is roughly linearly related to the near surface humidity q_{air} (e.g. Rapti 2005), which is estimated by a linear regression from ECHAM5 simulations scaled by topography:

$$VIWV_{atmos} = e^{-z_{topo}/z_{atmos}} \cdot 2.6736 \cdot 10^3 [\mathrm{kg/m^2}] \cdot q_{air} \quad (8)$$

Note, that the additional scaling by the topography should simulate the effect of nearly exponentially decreasing atmospheric water vapor mixing ratios. Changes per unit time in q_{air} by evaporation, Δq_{eva}, are given with the help of Eq. 7:

$$\Delta q_{eva} = \frac{-F_{latent}}{L} \cdot \frac{1}{2.6736 \cdot 10^3 [\mathrm{kg/m^2}]} \quad (9)$$

The latent heat release, Q_{latent}, in the atmosphere due to changes in q_{air} by condensation or precipitation, Δq_{precip}, is given by

$$Q_{latent} = -2.6736 \cdot 10^3 [kg/m^2] \cdot \Delta q_{precip} \cdot L \quad (10)$$

The condensation or precipitation, Δq_{precip} is assumed to be proportional to q_{air}

$$\Delta q_{precip} = r_{precip} \cdot q_{air} \quad (11)$$

with $r_{precip} = -0.1/24$ h, which corresponds to an autoregressive model with a decorrelation (recirculation)

time of about 14 days. It thus mimics the rough estimate of the mean lifetime of water vapor in the atmosphere. The complete tendencies of q_{air} are given by

$$\frac{dq_{air}}{dt} = \Delta q_{eva} + \Delta q_{precip} + \kappa \cdot \nabla^2 q_{air} - \vec{u} \cdot \nabla q_{air} + \Delta q_{correct} \tag{12}$$

with the changes in q_{air} given by Δq_{eva}, Δq_{precip}, the atmospheric circulation terms of isotropic diffusion and advection and the empirical flux correction term, $\Delta q_{correct}$, to correct for model climatology errors.

3.4 Sensible heat and atmospheric temperature

The sensible heat flux between the surface and the atmosphere can be approximated by Newtonian coupling:

$$F_{sense} = c_{atmos}(T_{atmos} - T_{surf}) \tag{13}$$

with the coupling constant $c_{atmos} = 22.5$ W/K/m^2 (following from Barsugli and Battisti 1998 minus the thermal radiation damping effect of about 2.5 W/K/m^2) and the atmospheric temperature, T_{atmos}. T_{atmos} itself is a prognostic variable following the tendency equation:

$$\gamma_{atmos}\frac{dT_{atmos}}{dt} = -F_{sense} + Fa_{thermal} + Q_{latent} + \gamma_{atmos}(\kappa \cdot \nabla^2 T_{atmos} - \vec{u} \cdot \nabla T_{atmos}) \tag{14}$$

The tendencies of T_{atmos} depend on the sensible heat exchange with the surface, F_{sense}, the net thermal radiation of the atmosphere, $Fa_{thermal}$, the latent heat release by condensation of atmospheric water vapor, Q_{latent}, and the two atmospheric circulation terms of diffusion and advection. The atmospheric heat capacity, γ_{atmos}, is chosen as the equivalent of a 5,000 m air column. The atmospheric absorption of solar radiation is neglected, as it is considered to be of minor importance in the context of this study.

The net thermal radiation of the atmosphere *is given by:*

$$Fa_{thermal} = \varepsilon_{atmos}\sigma \cdot T_{surf}^4 - 2\varepsilon_{atmos}\sigma \cdot T_{atmos-rad}^4 \tag{15}$$

The atmosphere absorbs thermal radiation from the surface relative to its emissivity and radiates to space and the surface. However, the radiation temperature $T_{atmos\text{-}rad}$ is different from T_{atmos}, as it need to be considered that the slab greenhouse model radiates in the atmospheric layer with the temperature of $0.84{*}T_{surf}$ independent of the emissivity (Bohren and Clothiaux 2006), while T_{atmos} following from Eq. 14 would be much warmer than that, since this equation does not consider adiabatic cooling by expansion with decreasing pressure. Thus our modeled T_{atmos} is roughly a potential temperature. To incorporate the much colder radiation temperature $T_{atmos\text{-}rad}$ we shift $T_{atmos\text{-}rad}$ relative to T_{atmos} by a constant: $T_{atmos\text{-}rad} = T_{atmos}$ $-0.16{*}\mathrm{T_{surf}}$(control) -5 K. The shift by -5 K results from the fact that the T_{atmos} following from Eq. 14 is in global mean average warmer than T_{surf} by about 5 K due to latent heating. Subsequently, $T_{atmos\text{-}rad} = 0.84{*}T_{surf}$ in the global mean of the control simulations, but changes in $T_{atmos\text{-}rad}$ in the scenario run are only a function of T_{atmos} (not T_{surf}). Thus $T_{atmos\text{-}rad}$ simulates a higher level atmosphere temperature that radiates to space and that follows the evolution of T_{atmos}.

3.5 Atmospheric circulation

The atmospheric circulation in the GREB follows a seasonal climatology and is assumed to not respond to external forcings. It thus represents a fixed boundary condition. The mean circulation, $\vec{u}$, is following the seasonally varying climatology of the NCEP reanalysis 850 hPa winds. The atmospheric transport is simulated by advection with $\vec{u}$, and isotropic diffusion with an effective diffusivity of $\kappa = 8 \times 10^5$m^2/s. The effective diffusivity κ roughly mimics the lifetime of a typical weather system, where disturbances with a radius of about 1,000 km have a lifetime of about a week, which is assumed to be the main cause of isotropic diffusion in the troposphere.

The contributions of neighboring grid points to the gradient and divergence operators in Eqs. 12 and 14 are scaled by topography (analog to Eq. 8), to incorporate some effect of the topography onto the circulation. Subsequently, it slightly reduces the contribution of high topographic regions to the circulation terms. The isotropic diffusion is additionally scaled by the local topography with the scaling height z_{topo} for the diffusion of heat and a smaller scaling height $z_{topo} = 5{,}000$ m for the diffusion of water vapor, which is assumed to be more strongly affected by topography, because air masses passing topographic features are generally precipitating some of the water vapor content, leading to a drying of the air mass.

3.6 Sea ice

The effect of changes in sea ice cover is only considered in the changes of the effective heat capacity γ_{surf}, which changes from the oceans mixed layer values to a 2 m water column over a transition temperature interval, see Fig. 3b. The change in heat capacity goes parallel with the change in the albedo (Fig. 3a). Latent heat releases by freezing and melting are neglected.

3.7 Deep ocean

A fraction of the heat gained by the surface layer of the ocean is mixed into the deeper and abyssal ocean, which is

important for considering the seasonal cycle and transient effects of climate change. This is simulated in the GREB model by a subsurface ocean layer:

$$\frac{dT_{ocean}}{dt} = \frac{1}{\Delta t}\Delta To_{entrain} - \frac{1}{\gamma_{ocean} - \gamma_{surf}} Fo_{sense} + Fo_{correct} \tag{16}$$

The tendencies of the subsurface ocean temperature, T_{ocean}, is given by the heat exchange with the surface ocean layer due to decreasing of the mixed layer depth, $\Delta To_{entrain}$, for a time step, Δt, turbulent mixing with the surface ocean layer, Fo_{sense}, and by a tendencies correction term, $Fo_{correct}$, which is an empirical correction of the tendencies of T_{ocean} to correct for model drifts. The climatological mean is forced to be the minimum of T_{surf}. Note, that the absolute values of T_{ocean}, are irrelevant, since only temperature differences to T_{surf} are needed. The effective heat capacity of the ocean, γ_{ocean}, is assumed to be a function of the mean maximum mixed layer depth $z_{ocean} = 3*\max(h_{mld})$, which ranges roughly between 100 and 1,000 m. Note that the heat exchange with deeper ($>z_{ocean}$) abyssal ocean is not simulated in the GREB model. A decreasing h_{mld} leads to entrainment of surface layer water, which results into $\Delta To_{entrain}$ of

$$\Delta To_{entrain} = \frac{-\frac{1}{2}\Delta h_{mld}}{z_{ocean} - h_{mld}}(T_{surf} - T_{ocean}) \tag{17}$$

with the change in the mixed layer depth, Δh_{mld}. An increasing h_{mld} leads to an entrainment of subsurface water into the mixed layer, which results into T_{surf} tendency, $\Delta T_{entrain}$, of

$$\Delta T_{entrain} = \frac{\frac{1}{2}\Delta h_{mld}}{h_{mld}}(T_{ocean} - T_{surf}) \tag{18}$$

Note that the factor ½ results from the finite temperature gradient below the mixed layer, which effectively leads to less entrainment than in a simple two layers step model. The turbulent mixing between the two ocean layers, Fo_{sense}, is simulated by a Newtonian coupling:

$$Fo_{sense} = c_{ocean} \cdot \left(T_{ocean} - T_{surf}\right) \tag{19}$$

with the coupling constant $c_{ocean} = 5$ W/K/m^2. The net heat flux from the deeper ocean to the surface layer is given by

$$F_{ocean} = Fo_{sense} + \gamma_{surf} \cdot \Delta T_{entrain} \tag{20}$$

3.8 Flux corrections

Simple climate models such as the one described above cannot simulate the mean state climate with sufficient accuracy. Simple conceptual models or EMICs will usually empirically optimize parameters or add additional flux corrections to the tendency equations to maintain a realistic climate. In many studies with simplified models modest mean state errors (in the order of several to 10 K) are accepted and are assumed to be of minor importance (e.g. Weaver et al. 2001, or Ganopolski et al. 2001). The T_{surf} tendency Eq. 1 without the flux correction term, $F_{correct}$, would result into a large model drift, with a root mean square error (RMS-error) of about 10 K (if the atmospheric water vapor is kept at climatological values). To maintain a mean climate state as observed, the simple climate models need to be empirically corrected. We chose to put all empirical corrections into the flux correction term $F_{correct}$ for T_{surf} tendencies, $Fo_{correct}$ for T_{ocean} tendencies and $\Delta q_{correct}$ for q_{air} tendency, which are estimated by calculating the residual tendencies needed to maintain the observed climatologies of T_{surf}, T_{ocean} and q_{air}. As a result the GREB model climatologies of T_{surf} and q_{air} are by construction identical to the observed ones. The advantage is that we can control the mean state climate directly and estimate the role of mean state biases. The disadvantage is that these flux corrections may potentially affect the climate sensitivity in a non-linear way. However, many studies have addressed climate sensitivities with using flux corrections in simplified ocean model to maintain a climate state close to the observed and most these study found the climate sensitivity in the these flux corrected GCMs is close to those of the not flux corrected simulations (e.g. Murphy et al. 2004 or Webb et al. 2006).

However, for further development of the model it is necessary to improve some of the solar and thermal radiation parameterizations, as discussed in the analysis and discussion below. For sensitivity experiments discussed in the analysis following below, the correction terms $F_{correct}$, $Fo_{correct}$ and $\Delta q_{correct}$ are recalculated for each experiment to maintain the observed climatologies. The full GREB model (EXP-10, see Table 3) has the smallest contribution of the flux corrections to the tendencies in T_{surf} and in the simplest experiment, where most processes are "turned off" (EXP-1), the flux corrections have the largest contribution to the tendencies. However, in all simulations the flux corrections are important to maintain a climate close to the observed and the global mean flux is not zero, as the model does not give a complete simulation of the atmosphere and ocean (e.g. it is missing resolved clouds or adiabatic atmospheric cooling).

3.9 Performance and limits

The GREB model as described above is numerically integrated on a horizontal grid with a 3.75° × 3.75° horizontal resolution and a numerical time step of 12 h (daily cycle is not resolved), except for the diffusion and advection schemes, which need a shorter time step for numerical

Table 2 Model parameters used in the GREB model, which are not standard literature values

Model parameter	Meaning
$z_{atmos} = 8{,}400$ m	Scaling height of the atmosphere
$z_{topo} = 5{,}000$ m	Scaling height for water vapor; only for isotropic diffusion
$c_{atmos} = 22.5$ W/K/m^2	Coupling parameter for turbulent heat exchange between T_{surf} and T_{atmos}
$\kappa = 2{\cdot}10^5$ m^2/s	Isotropic diffusion coefficient
$r_{precip} = -0.1/24$ h	Precipitation strength
$z_{ocean} = 3$*max(h_{mld})	Depth of the ocean
$c_{ocean} = 5$ W/K/m^2	Coupling parameter for turbulent heat exchange between T_{surf} and T_{ocean}
$pe_1 = 9.07211$/ppm, $pe_2 = 106.7252$ m^2/kg, $pe_3 = 61.5562$, $pe_4 = 0.0179$, $pe_5 = 0.0028$, $pe_6 = 0.0570$, $pe_7 = 0.3462$, $pe_8 = 2.3406$, $pe_9 = 0.7032$, $pe_{10} = 1.0662$	Parameters of the effective emissivity, ε_{atmos}, model

stability depending on the latitudes. The FORTRAN-code of the model is available as supplemental material. In the Appendix 1 the model's prognostic, diagnostic and climatic constants and the model parameters are listed, see Tables 1 and 2. The GREB numerical code computes one model year in a few seconds and a 200 years A1B-scenario in less than an hour on a standard personal computer. It therefore is a relatively fast tool, which allows conducting sensitivity studies to external forcing within minutes to hours.

Figure 5 shows the ensemble mean response in the A1B scenario (transient CO_2 concentration) of 24 models of the IPCC assessment report 4 (AR4) (Meehl et al. 2007a, b) for winter and summer in comparison with the GREB model response for the same scenario. We can note that the large-scale features of both models are similar, with a stronger warming over land (land-sea warming ratio), a polar winter amplification and a stronger warming on the Northern compared to the Southern Hemisphere. The seasonal differences in the response are also similar in both models, with a mostly stronger warming in the cold season.

Figure 6 shows the difference in the T_{surf} response pattern between the IPCC-ensemble mean and the GREB model. The global mean warming is about the same for both responses. It need to be noted, though, that the emissivity function of the GREB model has been fitted to agree with the global mean characteristics of the IPCC models, which to some degree enforces a good agreement with IPCC models on the global mean warming, but does not necessarily have to get the right regional differences. The most striking difference is over the arctic in winter, where the GREB model does not warm as much as the IPCC models. Further we can see a quite regional overestimation of the warming over the northern North Atlantic, which may most likely be related to the thermohaline circulation slow down in the IPCC simulation, which is not simulated in the GREB model. There seems to be some

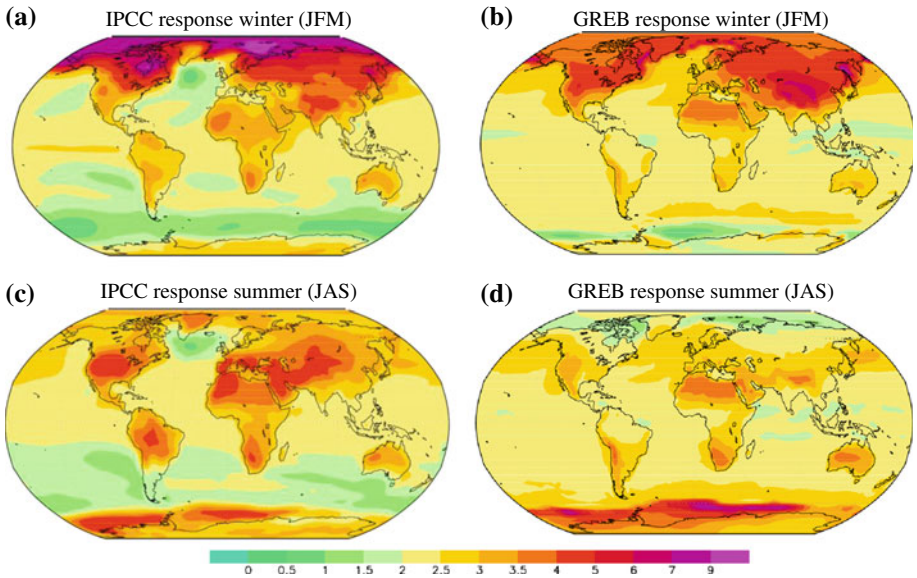

Fig. 5 A1B-scenario T_{surf} response in the IPCC ensemble mean (*left*) and the GREB model (*right*) for winter (*upper*) and summer season (*lower*). The response is defined as the T_{surf} difference between the time intervals 2070–2100 and 1970–2000 in (K)

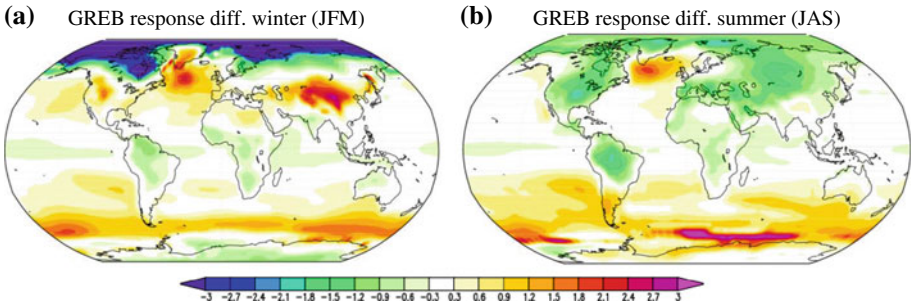

Fig. 6 T_{surf} response difference of the GREB model (EXP-12) relative to the IPCC ensemble mean, in [K]

indication that the regions with strong ice-albedo feedbacks (see Fig. 3) tend to warm too much (e.g. the northern hemisphere midlatitudes winter continental regions). The southern ocean is another region, in which the GREB model warms too much. Further there is some indication that the summer continental regions do not warm as much in the GREB model as they do in the IPCC simulations.

The response difference of the GREB model relative to the IPCC ensemble mean response can be compared with the response differences of the individual IPCC ensemble members relative to the IPCC ensemble mean. The model uncertainties may be quantified in terms of the global mean climate sensitivity and the uncertainty in the regional amplitudes of the response pattern,[1] see Fig. 7. The IPCC models build an uncertainty cloud with a global mean climate sensitivity of about 2–3 K and a mean regional amplitude uncertainty of about 20–35%. The GREB model is within this model uncertainty cloud, but with relatively large deviation from the IPCC ensemble mean response pattern.

Since the T_{surf} response strongly depends on the response in T_{atmos}, q_{air} and T_{ocean}, it is worth looking at the response of these quantities to further verify the skill of the GREB model. Figure 8 shows the response to $2 \times CO_2$ in T_{atmos} relative to T_{surf}, in relative humidity, the ocean heat uptake and the change in precipitation. Over the tropical ocean the response in T_{atmos} is about 20% larger than the response in T_{surf}, which is due to the latent heat release in the atmosphere. In higher latitudes and on land the response in T_{atmos} is about the same as in T_{surf}. The overall effect is roughly consistent with the T_{atmos} response found in the IPCC-models (Meehl et al. 2007a, b).

[1] The uncertainty in the local response amplitude can be estimated by the normalized response pattern RMS-error of each model relative to the normalized IPCC ensemble mean response pattern:

$$\sigma_i = \sqrt{\sum_{x,y}\left(\frac{T_i(x,y)}{\hat{T}_i} - \frac{T_{ensemble}(x,y)}{\hat{T}_{ensemble}}\right)^2_{winter} + \sum_{x,y}\left(\frac{T_i(x,y)}{\hat{T}_i} - \frac{T_{ensemble}(x,y)}{\hat{T}_{ensemble}}\right)^2_{summer}}$$

with the T_{surf} response of the individual Models, T_i, and that of the IPCC ensemble mean, $T_{ensemble}$, and their respective global winter and summer means, $\hat{T}_i$ and $\hat{T}_{ensemble}$. The normalized response pattern RMS-error of each model, ε_i, gives a measure of the relative uncertainty of the local response amplitudes, independent of the global mean response.

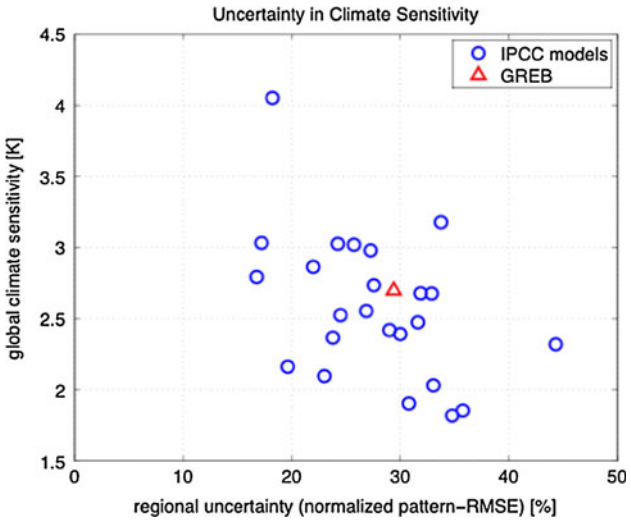

Fig. 7 Scatter plot of the models climate sensitivity for the A1B-scenario. The x-axis shows an estimate of the mean local response amplitude deviation from the IPCC-ensemble mean response, σ_i (see text for a definition), as a measure of regional differences in the warming pattern and the y-axis the global mean T_{surf} response

In the GREB model the deep ocean heat uptake is basically a function of the mixed layer depth and the surface warming. The ocean heat uptake is mostly confined to northern midlatitudes and a band in the southern ocean, due to the larger mixed layer depths in these regions. The spatial pattern and amplitude is roughly comparable with findings in CGCM studies (Banks and Gregory 2006).

The relative humidity is unchanged for most oceanic region, but shows a small decrease in northern continental regions, which seems to be in good agreement with GCM studies (see Held and Soden 2000). The change in precipitation can be estimated by the change in Δq_{precip}, although it needs to be noted that the simplistic representation of condensation or precipitation in the GREB model does not allow for reduced precipitation by increased temperatures. However, the global mean increase of about 10% and the large scale structure, with stronger relative increase in precipitation with increasing latitudes and over land is comparable to that found in the IPCC models (Meehl et al. 2007a, b). The decrease in precipitation found

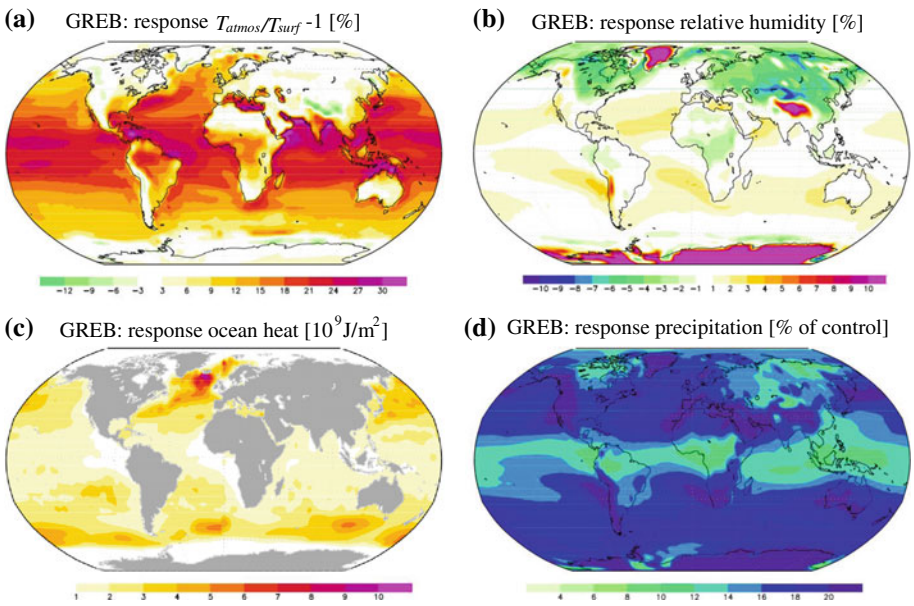

Fig. 8 The GREB model response to 2 × CO_2 after 50 years (EXP-10) in T_{atmos} relative to T_{surf} (**a**), the relative humidity (**b**), the ocean heat uptake (**c**) and the response in precipitation as estimated by changes in Δq_{precip} (**d**)

in the subtropical regions in the IPCC-models cannot be simulated with the GREB model.

4 Conceptual understanding of climate sensitivity

We will now discuss some large-scale aspects of the climate response to anthropogenic greenhouse gas forcings. The simplicity of the GREB model allows deconstructing the climate change response pattern by not simulating individual processes. We therefore build a series of sensitivity experiments, in which elements of the GREB model are '*turned off*', to illustrate how different feedbacks produce different structures of the global warming response pattern. See Table 3 for a complete list of the sensitivity experiments. In all control experiments the control CO_2 concentration is 340 ppm and doubled for all sensitivity experiments. The flux correction terms are recomputed for each sensitivity experiments, in order to maintain the same mean state climate. It is important to note, that switching of some feedbacks can result into an unstable climate mean state (e.g. tropical water vapor feedback without interaction to the high latitudes (Pierrehumbert 1995)). We therefore discuss only sensitivity experiments, in which the climate mean state is stable (e.g. a small perturbation of the climate will lead back to a stable mean state). In the discussion it has to be noted that the processes and feedbacks are not linear. The relative influence of a process on the response pattern will in general depend on the other feedbacks as well (e.g. Bates 2007 or Cai and Lu 2009) The following discussion is therefore depending on the order in which processes are '*turned off*' or '*turned on*' and shall only give one perspective on a deconstruction of the climate response signals.

In the whole discussion following it needs to be noted that the GREB model is only a very simplified model, which may in many aspects get the relative importance of a process incorrect, neglect important aspects or may be producing the right response for the wrong reasons. The results should therefore be taken with some caution and should only give a rough idea of the main interactions.

4.1 Deconstructing the climate response

Figure 9 shows a series of T_{surf} response patterns starting with the sensitivity experiments where most processes are 'turned off' and ends with the full GREB model. For the simplest case (EXP-1) we can consider the response to a 2 × CO_2 increase where the only feedback is the thermal radiation response to changes in T_{surf} and where topography or regional differences in the atmospheric water vapor and cloud cover are not considered, see Fig. 9a. The T_{surf} response is a weakly monotonically increasing function of T_{surf} (compare Figs. 9a with 1c), because the thermal radiation emitted by the atmospheric greenhouse gases is proportional to T_{surf}^4 (see Eq. 3).

The effect of the topography, in the case where no feedbacks from atmospheric water vapor or snow and sea ice cover are considered (EXP-2), is to reduce the effective emissivity of the atmosphere due to the smaller optical thickness. Subsequently regions with higher altitudes will have a weaker local response to a CO_2 increase than low-altitude regions. This picture will however change substantially, when feedbacks from atmospheric water vapor or snow and ice cover and differences in mean water vapor are considered, as discussed further below.

Table 3 List of GREB model simulations

Experiment number and name	Length	Scenario	Global mean response	Land/ ocean	Arctic/ global	Description
1. No-feedbacks	50 years	$2 \times CO_2$	1.46	1.0	0.9	Only the thermal radiation response and not considering topography, atmospheric circulation or regional differences in the relative humidity or clouds. Topography over land is set to sea level/$q_{air} = 5.2$ g/kg globally constant and latent heat fluxes are replaced against flux corrections/cloud cover is 70% globally/sea ice distribution is fixed/diffusion and advection terms of the atmospheric circulation are set to zero
2. Topo-no-feedbacks	50 years	$2 \times CO_2$	1.46	1.0	0.9	As EXP-1, but with the true topography
3. Clouds-no-feedbacks	50 years	$2 \times CO_2$	1.48	1.0	0.9	As EXP-2, but with the true cloud cover
4. Humid-no-feedbacks	50 years	$2 \times CO_2$	1.39	1.1	1.0	As EXP-3, but with the true humidity
5. Circulation-No-feedbacks	50 years	$2 \times CO_2$	1.40	1.0	1.0	As EXP-4, but with the diffusion and advection terms of the atmospheric circulation considered for heat only (not for q_{air})
6. Ice-albedo	50 years	$2 \times CO_2$	1.51	1.1	1.1	As EXP-5, but with changes in the albedo and ice cover due to changes in T_{surf} as in Fig. 3
7. Local-Water–vapor	50 years	$2 \times CO_2$	2.56	1.1	1.1	As EXP-6, but with changes in q_{air} ($viwv_{atmos}$) and associated changes in F_{latent} and Q_{latent}
8. Water–vapor-diffusion	50 years	$2 \times CO_2$	2.67	1.2	1.2	As EXP-7, but with atmospheric transport of q_{air} by diffusion only
9. No-ocean	50 years	$2 \times CO_2$	2.62	1.3	1.3	All processes considered, but no heat exchange to the subsurface ocean
10. GREB	50 years	$2 \times CO_2$	2.51	1.3	1.3	All processes considered
11. Linear-emi-vapor	50 years	$2 \times CO_2$	2.65	1.1	0.9	As EXP-9, but $viwv_{atmos}$ in Eq. 4 is kept at the control values and another linear term is added to Eq. 4 with $+0.0061\frac{m^2}{kg} \cdot (VIWV_{atmos} - VIWV_{atmos}(control))$
12. A1B	1940–2100	A1B	2.70	1.3	1.3	CO_2 increase as in the IPCC A1B scenario
13. A1B-no-water–vapor	1940–2100	A1B	1.62	1.1	1.1	As EXP-6, but for the A1B-scenario and interaction with the subsurface ocean
14. SST + 1 K	5 years	Constant	1.01	1.0	1.0	SST is increased by 1 K relative to the control SST.
15. SST + 1 K No-water–vapor	5 years	Constant	0.90	0.7	1.1	As EXP-14, but with water vapor kept to climatological values (as in EXP-6)
16. SST + 1 K No water vapor transport	5 years	Constant	0.84	0.6	1.1	As EXP-15, but no transport of atmospheric water vapor (as in EXP-7)

Column 4 gives the global mean T_{surf} response in K. Column 5 and 6 give the ratio in T_{surf} response for Land/Ocean (ice free regions in control) and Arctic (north of 70°N)/global

The cloud cover has an effect onto both the solar and thermal radiation. In the absence of ice-albedo and water vapor feedbacks we can here discuss only the effect of the mean cloud cover on the local thermal radiation response, see Fig. 9d,e. Regions with relatively (to the mean of 70%) low cloud cover will have a stronger thermal radiation response (see Eq. 5), as can be seen, for instance over the Sahara or southern Africa. On the other hand regions with large cloud cover have a reduced local radiation response, as can be seen, for instance over the Southern Ocean.

The mean atmospheric water vapor, $viwv_{atmos}$, influences the response to a CO_2 increase by changing the mean emissivity and by changing the sensitivity to CO_2 changes, see Eq. 4. Regions with larger $viwv_{atmos}$ have a smaller sensitivity to CO_2 changes (see Fig. 4a) due to the overlap in the absorption wavelengths. This reduces the local response in the moist tropical regions substantially and increases the response over higher altitudes, see Fig. 9g. However, the change is not as strong as one may have expected from the strength of the sensitivity of ε_{atmos} to $viwv_{atmos}$ (see Fig. 4c), because an increase in the mean

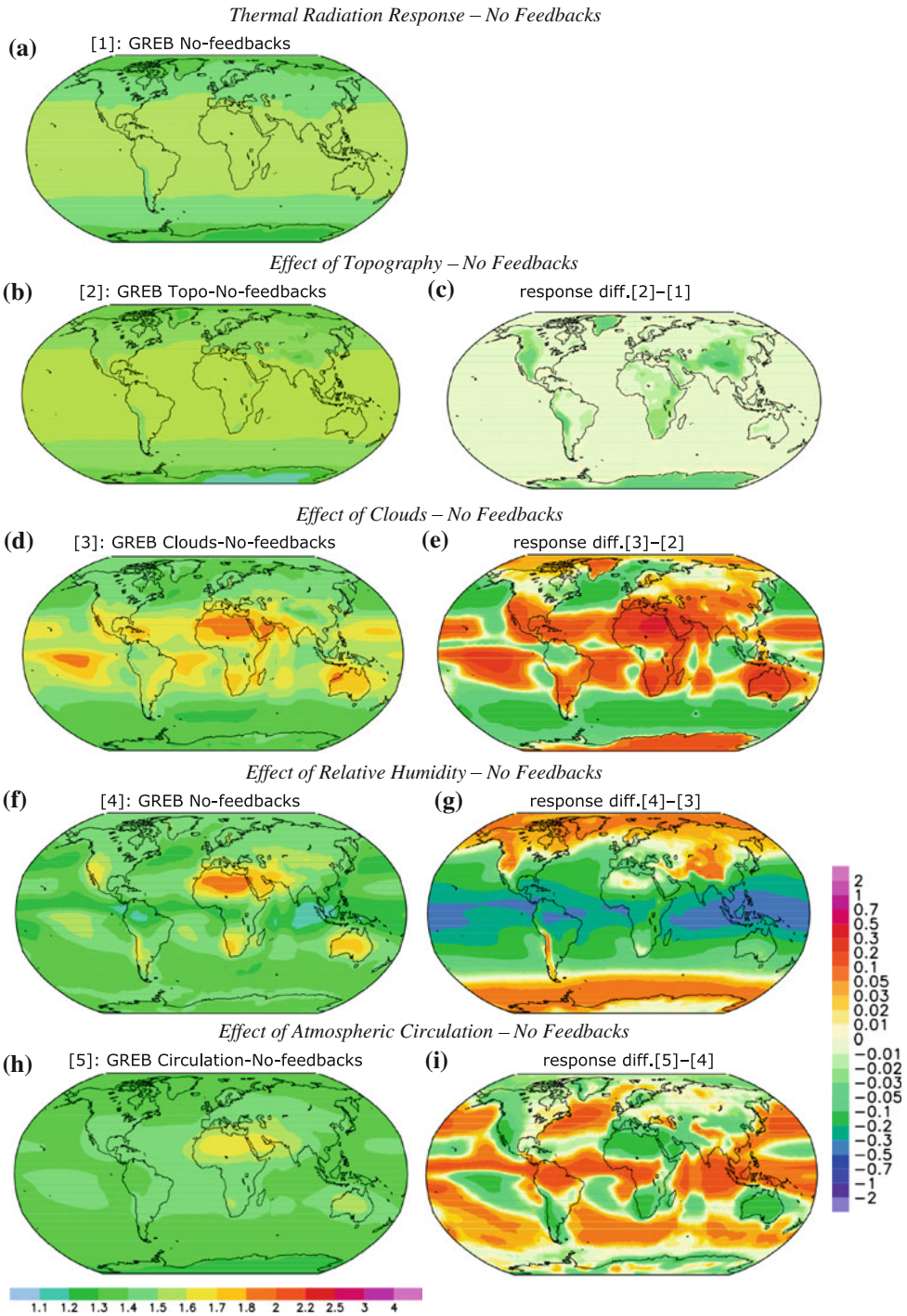

Fig. 9 The T_{surf} response to $2 \times CO_2$ increase after 50 years in a series of sensitivity experiments, in which different elements of the GREB model are 'turned off', starting with the simplest model and finishing with the complete GREB-model. The panels to the *right* show the response difference to the previous (row above) sensitivity experiment, in [K]

atmospheric water vapor, $viwv_{atmos}$, also increases the mean ε_{atmos}, which leads to an effectively weaker negative feedback to changes in T_{surf}. Subsequently regions with larger $viwv_{atmos}$ tend to have a stronger T_{surf} sensitivity for a given forcing than regions with low $viwv_{atmos}$.

The atmospheric circulation will advect and turbulently diffuse heat (thus changes in T_{surf}) from one region to neighboring regions. It effectively leads to a smoothing of the response pattern (Fig. 9h). The stronger warming over subtropical oceans, dry, warmer and low altitude regions is transported to the wet, warm tropics, continental and high altitude regions, see Fig. 9i.

The first main feedbacks that amplify the response to CO_2 increase are the ice/snow-albedo and the sea ice cover feedbacks, which mostly affect the higher latitudes (see Fig. 9j, k). Both feedbacks together lead to a warming of

Fig. 9 continued

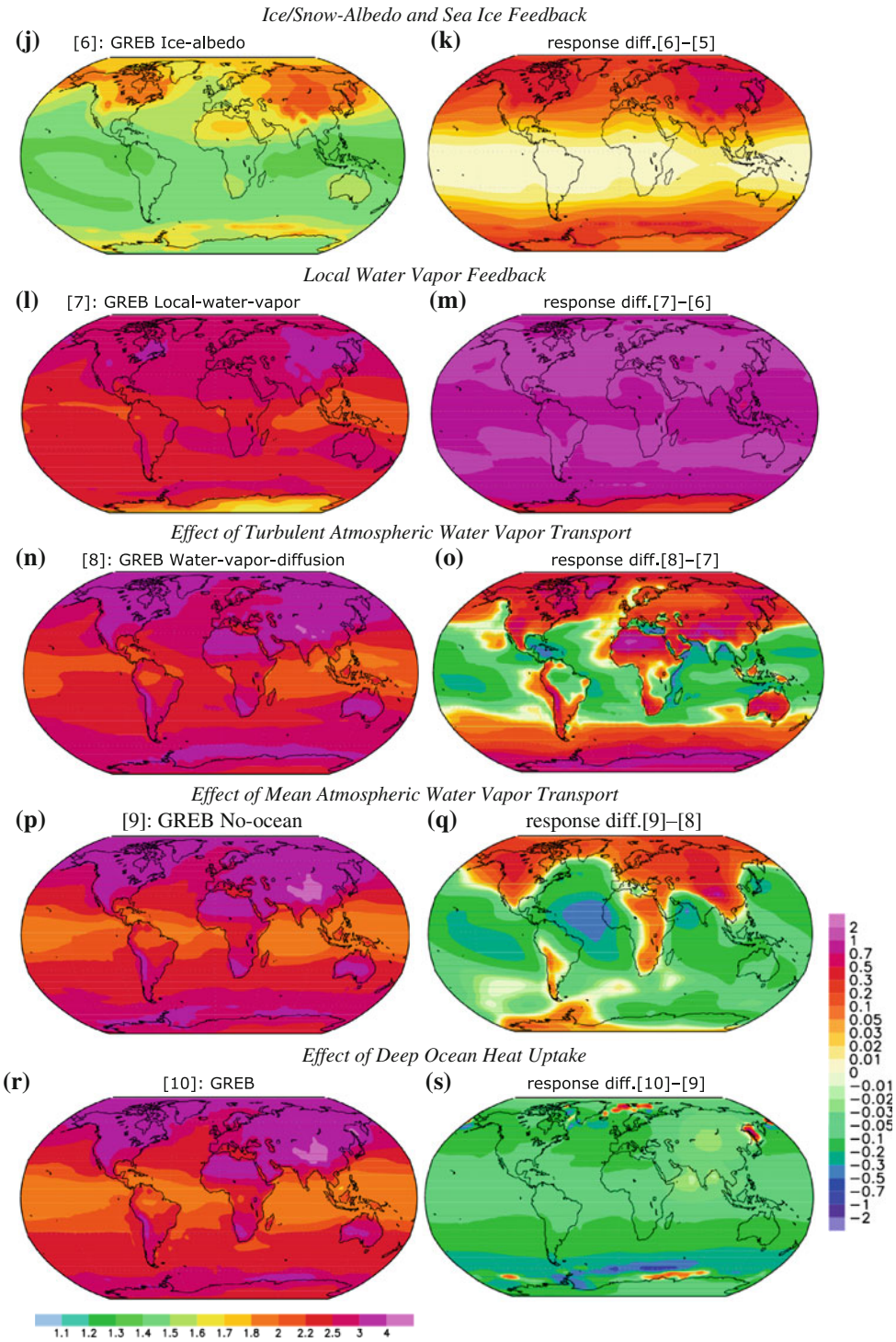

the northern hemisphere high latitudes that is stronger than the warming anywhere else. In the southern hemisphere the warming is not as strong, because large continental regions with the mean T_{surf} in the range of the strong snow-albedo feedback (see Fig. 3c, d) are missing.

The response of the atmospheric water vapor $viwv_{atmos}$ to increased T_{surf} is the main positive feedback for the climate warming globally, see Fig. 9l. Note that the effect of the water vapor response is strong also in the northern mid to high latitudes, despite the fact that the evaporation of water vapor is strongest in the tropics. This is to some extent caused by the combined effects of the snow/ice-albedo, the sea ice cover and the radiative water vapor feedbacks. The later is related to the non-linear dependency

of the ε_{atmos}-function to atmospheric water vapor $viwv_{atmos}$, which causes the thermal downward radiation to be more sensitive to changes in $viwv_{atmos}$, when the values of $viwv_{atmos}$ are smaller, see Fig. 4.

The atmospheric circulation transports water vapor by the mean circulation and by turbulent mixing (Fig. 9n–q). Both processes lead to a further amplification of the warming response in higher latitudes and a damping (or cooling) of the response in the tropical regions. The turbulent mixing of $viwv_{atmos}$ will lead to an increase in $viwv_{atmos}$ in regions were the mean $viwv_{atmos}$ is relatively small (compare Figs. 1d and 9o). These are desert, cold and high altitudes regions. The cold high-altitudes desert of Antarctica shows therefore a strong response to the turbulent transport of water vapor. The advection of $viwv_{atmos}$ plays a role where the mean winds (see Fig. 1e) blow against strong $viwv_{atmos}$ gradients (see Fig. 1d). In the northern hemisphere this process is quite effective and amplifies the response in the high latitudes and polar regions, while at the same time it damps the warming of the tropical regions substantially (Fig. 9q). In the southern hemisphere this effect is not as strong due to the mostly zonal structure of the mean wind field.

Finally we can consider the effect of heat exchange with the deeper oceans on the T_{surf} response, see Fig. 9r, s. Quite obviously the effect is that of a global damping of the T_{surf} response, which is strongest where the warming was strongest. However, the damping effect is stronger over the southern Ocean due to the relative large ocean and the relative strong mixing here (compare with Fig. 1h). Note, that the overall heat uptake of the deeper ocean is not easily identified from Fig. 9s, but is shown in Fig. 8c.

4.2 The land-sea warming contrast

One of the most significant features of the T_{surf} response pattern is the stronger warming over land than over oceans, which is an intrinsic feature of climate dynamics that persists even in the equilibrium $2 \times CO_2$ response. The land-sea warming ratio in the IPCC simulations ranges between 1.4 and 1.8 with a mean of 1.6 in the transient A1B-scenario and between 1.2 and 1.6 with a mean of 1.3 in the equilibrium $2 \times CO_2$ scenario (Sutton et al. 2007). The GREB model has a comparable land-sea warming ratio with 1.3 (A1B scenario) and 1.3 (equilibrium $2 \times CO_2$), respectively.

We can again use the GREB model to deconstruct the feedbacks causing the land-sea contrast. The snow-albedo effect has a significant amplification of the warming response mostly over the northern continents. We can further note in Fig. 9o, q that the atmospheric circulation of water vapor plays a key role in the land-sea contrast. The combined effects of the water vapor response processes, clearly forces the land-sea contrast, especially in the warmer continental regions. The transient A1B-scenario without the water vapor feedbacks (EXP-13) has a much weaker land-sea warming ratio of 1.1, compared to 1.3 if all feedbacks are included.

To further illustrate the amplified land response to the ocean warming a set of sensitivity experiments is carried out, in which the SST is warmed uniformly by +1 K without CO_2 forcing and additionally some feedback processes are 'turned off', see response patterns in Fig. 10. These experiments are in reference to the previous studies (e.g. Cess et al. 1990 Joshi et al. 2008 and Dommenget 2009). In the first experiment, where the atmospheric water vapor, $viwv_{atmos}$, is not allowed to respond, the warming over land is much weaker than over oceans and is essentially caused by advection of warmed ocean atmospheric temperatures, with some positive feedbacks at high latitudes due to the ice-albedo feedback, see Fig. 10a. If the local $viwv_{atmos}$ is allowed to respond to changes in T_{surf}, but water vapor is not allowed to be transported by the atmospheric circulation, then the response over land is much stronger, see Fig. 10b. The response in local $viwv_{atmos}$ over the warm oceans is warming T_{atmos} by more than 1 K by latent heat release (see Eq. 14 and Fig. 8a) in the tropics, which leads to the advection of heat to the continental regions. Over land the local water vapor and in higher latitudes the ice-albedo feedbacks additionally amplify the T_{surf} response. Finally, if the response in $viwv_{atmos}$ is transported by the atmospheric circulation (Fig. 10c), the additional $viwv_{atmos}$ over land causes a further amplification of the land warming, leading to the nearly global signature of the land warming more than the oceans, which supports the findings of Dommenget (2009).

The above deconstruction of the land-sea warming contrast indicates that the strong continental warming is essentially an amplified response to the oceans warming. This has, as discussed in Dommenget (2009), implications for natural variability as well and explains why prescribing observed SSTs of the past century (Zhang et al. 2007; Compo and Sardeshmukh 2009; Dommenget 2009) can reproduce much of the continental warming.

4.3 The polar amplification

The strongest response to changes in CO_2 is in the arctic during winter, see Fig. 5. This is in most studies attributed to the ice/snow-albedo and sea ice cover feedback (e.g. Manabe and Stouffer 1980; Serreze and Francis 2006 or Meehl et al. 2007a, b). The GREB model response is similar to the IPCC ensemble mean response in the northern high latitudes, but also has some differences. The Polar regions are shown in more detail in Fig. 11. While both the IPCC and the GREB response are strongest in wintertime, the GREB model has a more pronounced

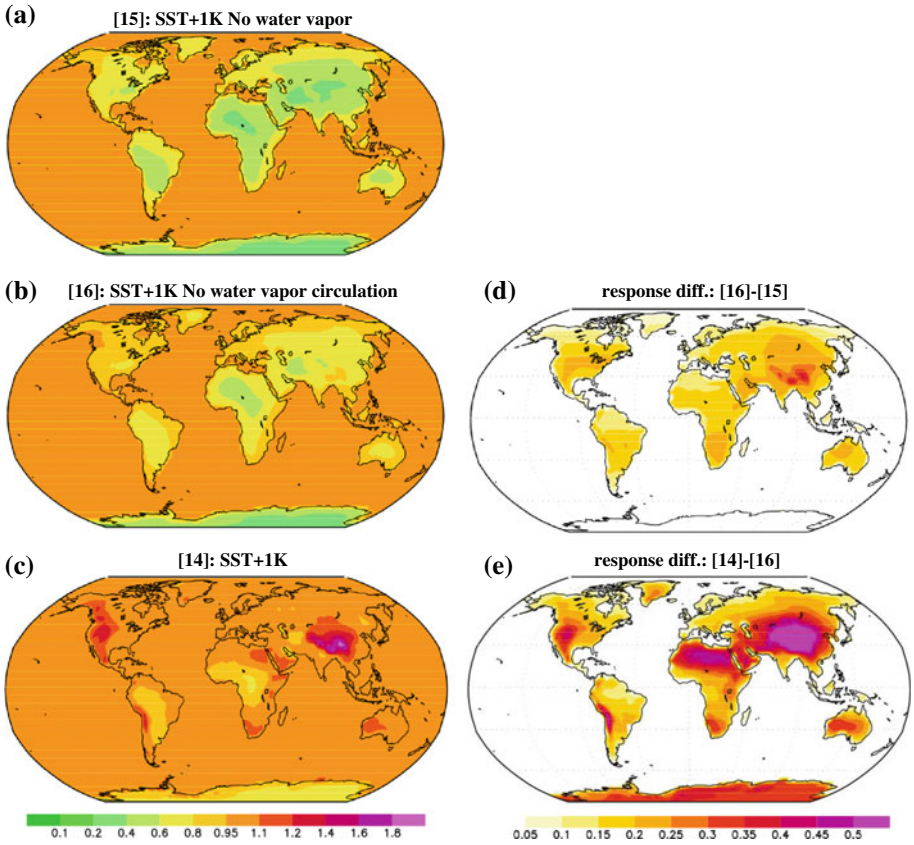

Fig. 10 T_{surf} response (after 5 years) to a 1 K warming of the SST in different GREB sensitivity experiments, see text and Table 3 for details

response at the ice edges and not such a strong response in the arctic sea (it is weaker than in the midlatitudes). However, overall the GREB model still produces some arctic wintertime amplification. We can therefore use the GREB model to deconstruct the arctic region response, while keeping in mind that some significant limitations in the GREB model exist for this region, indicating that some important feedback may me missing or are insufficiently simulated in the GREB model.

First we can recognize that the snow-albedo feedback is the strongest in the wintertime over the continental regions around 40°–50°N, see Fig. 3c. The feedback does not affect regions further north due to the weaker solar radiation and due to the much colder mean T_{surf} in winter, which does not allow melting (and associated change in albedo) of snow. The changes in sea ice cover are strongest in the fall seasons (not shown) and mostly affect the boundaries of the winter time ice cover, because the temperatures further north are too cold, which is in general agreement with other GCM studies (e.g. Manabe and Stouffer 1980).

The atmospheric water vapor feedback contributes significantly to the arctic amplification in the GREB model as illustrated by Fig. 9m, o, q. The figures illustrate that the combined feedbacks of snow-albedo, sea-ice cover, local water vapor and atmospheric circulation of water vapor create the polar amplification. It is interesting to note that the transport of water vapor alone has some significant arctic warming (see Fig. 9o, q). This is partly owed to the non-linear relationship between ε_{atmos} and $viwv_{atmos}$ in Eq. 4.

To illustrate this non-linear effect we conducted another sensitivity experiment, in which we kept $viwv_{atmos}$ in Eq. 4 at the control climate and added another linear term to Eq. 4 with $+0.0061\frac{m^2}{kg} \cdot (VIWV_{atmos} - VIWV_{atmos}(control))$, which simulates a linear response to increased $viwv_{atmos}$ in Eq. 4, which corresponds to about the same global mean change in emissivity as in the original Eq. 4 for a $2 \times CO_2$ scenario. The T_{surf} response is now stronger in the tropical regions and weaker in the high latitudes (see Fig. 12). Unlike the CO_2, which is globally well mixed and therefore constant, the atmospheric water vapor levels are strongly depending on temperature, the potential availability of water due to surface wetness and to the atmospheric circulation. The non-linear dependence of ε_{atmos} on $viwv_{atmos}$ in Eq. 4 makes the local water vapor feedback stronger over cold and dry regions. It thus contributes to the polar amplification and to the land-sea contrast in the GREB model. The results appear to be in general agreement with a recent GCM study by Graversen and Wang (2009), which also pointed out that

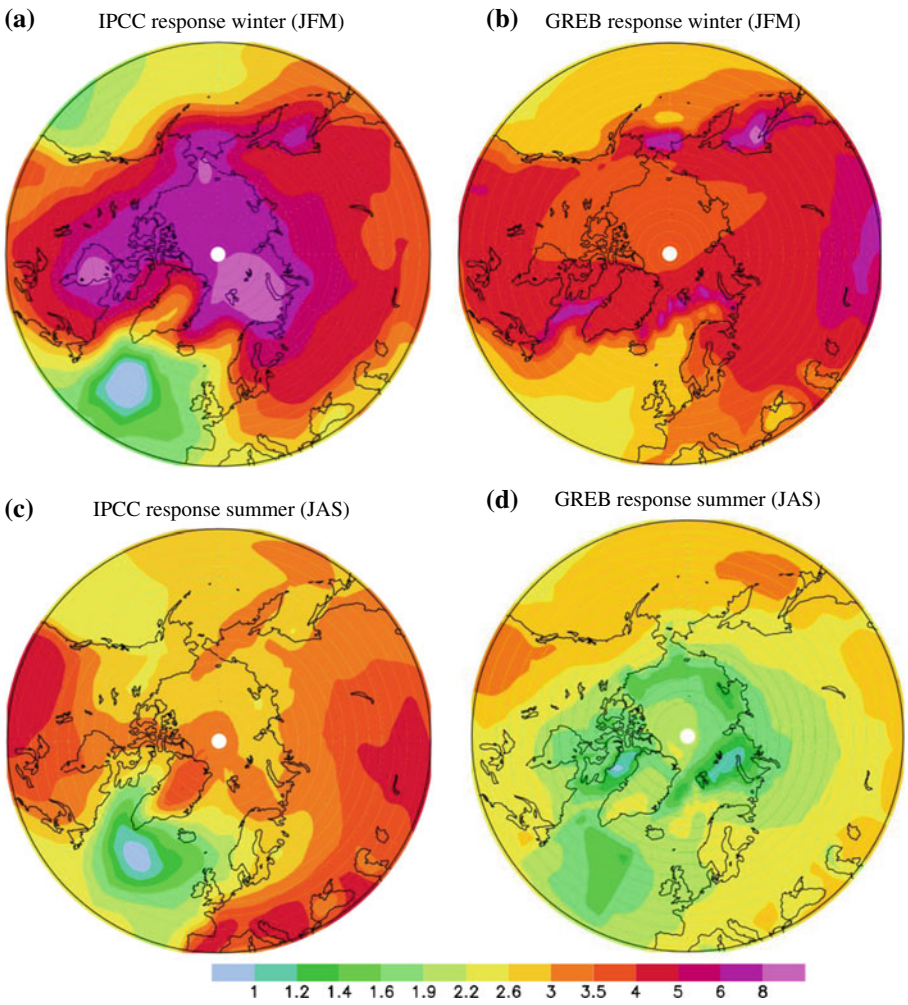

Fig. 11 As Fig. 5, but from a north polar view. Values are in Kelvin

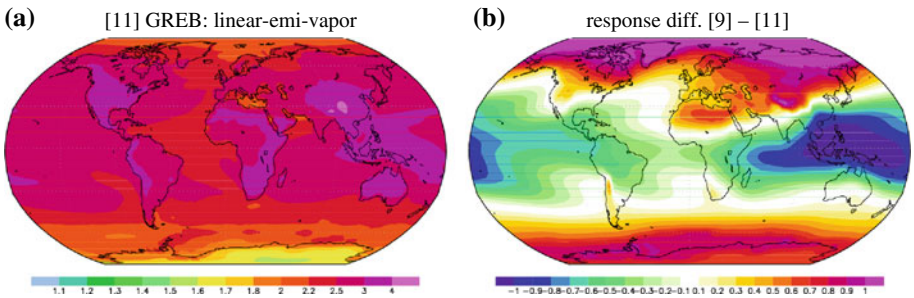

Fig. 12 The T_{surf} response in a sensitivity experiment with the GREB-model (EXP-11), in which ε_{atmos} is a linear function of the $viwv_{atmos}$ response in Eq. 4. The *right panel* shows the response different relative to the GREB EXP-9

the water vapor feedback contributes significantly to the polar amplification.

We noted that the polar climate and its response to external forcing are strongly depending on the climate of remote regions and their response to the external forcing. The polar amplification is not as clear and strong in the southern hemisphere as it is in the arctic for several reasons: Antarctica is surrounded by the Southern Ocean, which is not warming much, in contrast to the Arctic, which is surrounded by continents, which warm strongly due to different feedbacks as discussed above. Subsequently the Antarctic region is not warming as much as the Arctic. Further, Antarctica is mostly a high-altitude region, which is less connected to the atmospheric circulation of heat and water vapor, which is mostly affecting low-altitudes. The circulation effects cause a weaker response of the Antarctic than in the Arctic. Last, but not least, the Antarctic region is also more isolated from the tropical regions than the Arctic, by the more zonal atmospheric circulation in the southern hemisphere than in the northern hemisphere (see Fig. 1e).

This leads to weaker transport of water vapor by the mean atmospheric circulation and a subsequently weaker warming of the Antarctic region (see Fig. 9q).

5 Summary and discussion

In this study we introduced the strongly simplified climate model GREB. It simulates the globally gridded temperature resolved on three vertical layers (atmosphere, surface and subsurface ocean) and the atmospheric water vapor content in the atmospheric level. The model simulates, with strongly simplified physics, the solar and thermal radiation for the surface level, the hydrological cycle of surface evaporation and atmospheric condensation of water vapor and associated latent heat release, the turbulent sensible heat exchange between the three layers, the advection of heat and water vapor in the atmospheric layer by the mean atmospheric circulation and isotropic diffusion, changes in sea ice and land snow cover and the heat uptake of the deeper oceans. In contrast to CGCMs the model assumes a fixed atmospheric circulation, clouds and soil moisture, which are given as boundary conditions. It thus does not simulate internal chaotic climate variability caused by weather fluctuations and also assumes that climate change, due to external forcings such as $2 \times CO_2$ increase, is a small perturbation, which does not change the atmospheric or ocean circulation, which is clearly a simplification. Further the model's mean climatology in T_{surf} and q_{air} are corrected by flux corrections to follow the observed climatologies.

The main aim of the GREB model is to present a simple and fast tool, which helps to conceptually understand aspects of the climate system response to anthropogenic forcings or external forcings in general. It shall provide a basis or starting point to develop hypotheses about the processes involved in aspects of climate change or climate variability, which must than further be tested with observations or more complex and more realistic CGCM simulations.

Additional processes (e.g. clouds, soil moisture or atmospheric lapse rates) may in principle be simulated (or may be simulated more accurately) within the frame work of the GREB model, but in this first formulation of the GREB model the aim was to keep the model as simple as possible, but still be able to simulate the main large scale characteristics of the global warming response pattern. The GREB model as formulated here may therefore be regarded as a starting point to build in more detailed representations of some feedbacks, which were not included in this study or have been represented in very simplistic ways. The results of this study may already indicate, which processes may need further considerations.

The main findings of this study can be summarized to the following points:

(a) The simple GREB model gives a decent representation of the surface temperature response to global greenhouse gas increases. It can simulate the global mean climate sensitivity and large-scale regional aspects of the warming pattern within the uncertainty of the IPCC-model ensemble. The GREB-model response does not involve any atmospheric circulation changes, changes in cloud cover or any changes in the land surface moisture. However, the fact that the GREB-model agrees well with the IPCC-model ensemble shall not be interpreted as an indication that such effects are unimportant. Moreover it can be interpreted as an indication that such effects are very uncertain within the IPCC-model ensemble and that the IPCC-model ensemble response only represents those elements of the climate change pattern, on which all models agree relatively well. The simple GREB model will in many cases, regions or seasons give only a crude estimate of the response, neglecting some processes

Table 4 List of global mean emissivity characteristics assumed values and the models estimated

Characteristic	Assumed value	Model estimate
ε_{atmos} (current climate)	0.80 ± 0.03	0.80
$\Delta\varepsilon_{atmos}$ ($2 \times CO_2$)	0.019 ± 0.003	0.024
$\Delta\varepsilon_{atmos}$ ($\Delta viwv_{atmos}$)	0.02 ± 0.003	0.020
$\Delta\varepsilon_{atmos}(viwv_{atmos} \rightarrow 0)$	0.5 ± 0.1	0.49
$viwv_{atmos}$ spectral bands (Eq. 21)	0 ± 0.3	−0.07
$\Delta\varepsilon_{atmos}(CLD \rightarrow 0)$	0.16 ± 0.03	0.158
CO_2-$viwv_{atmos}$ overlap (Eq. 22)	0 ± 0.2	−0.20
CLD-sensitivity (Eq. 23)	0 ± 0.3	−0.14
$\Delta\varepsilon_{atmos}(CO_2 \rightarrow 0)$	0.18 ± 0.02	0.05
CO_2 spectral bands (Eq. 24)	0 ± 0.5	−1.5
$\varepsilon_{atmos}(CO_2 = CLD = viwv_{atmos} = 0)$	0 ± 0.3	−0.26
$\varepsilon_{atmos}(CLD = 1.0;\ viwv_{atmos} = 70\ \mathrm{kg/m^2})$	1.0 ± 0.3	1.0

that may indeed be the main factors for the regional changes in individual models or the real climate.
The largest uncertainty in the GREB model response to increased CO_2 concentrations is the downward thermal radiation response to changes in atmospheric water vapor or clouds. This may mainly result from the simple function used in Eqs. 4, 5 and the uncertainty in the ε_{atmos} parameter, which may mostly result from clouds and regional differences in the vertical temperature lapse rates. The results suggest that further improvement of the GREB model should focus on a better representation of the thermal radiation response, which will most likely focus on the effects of clouds and the lapse rates. Changes in the cloud cover may also contribute to feedbacks in the solar radiation, which are not considered in this model, but may potentially be important.

(b) The main large-scale features of climate change appear to be well understood as an interaction of some simple feedbacks. The advection of warmer temperatures and, most importantly, increased atmospheric water vapor to land and high latitudes leads to stronger warming in these regions. This is amplified by local water vapor feedbacks and the snow and sea ice cover feedbacks. An important aspect of the large-scale climate change pattern in the GREB model is the unequal distribution of mean atmospheric water vapor and the non-linear sensitivity of the thermal radiation to changes in atmospheric water vapor. This combination leads to strong climate sensitivity where the mean atmospheric water vapor levels are low (e.g. polar winter regions, continents or deserts). Regions of low water vapor levels are especially sensitive to transport of enhanced atmospheric water vapor.

(c) The land sea contrast in the GREB model is a combination of a transient effect due to the larger heat capacity of the oceans, the local positive feedbacks of water vapor and snow-albedo and the intrusion of water vapor from tropical oceans. The water vapor feedbacks do lead to the fact that continental climates are very sensitive to changes in the oceans T_{surf}. This may explain why atmospheric GCM simulation forced with observed SST only (no changes in greenhouse gases) can reproduce much of the continental warming (Zhang et al. 2007; Compo and Sardeshmukh 2009; Dommenget 2009).

(d) The polar amplification in the GREB model is not only a local response to changes in sea ice cover or snow albedo, but is also depending on the water vapor feedback. The latter is to a large degree a result of the non-linear sensitivity of the thermal downward radiation to increased atmospheric water vapor concentrations and also results from the fact that atmospheric water vapor is highly unequally distributed globally. Further, the water vapor feedback not only depends on the local water vapor response, but is strongly affected by the transport of water vapor from lower latitudes. The results appear to be in general agreement with a recent GCM study by Graversen and Wang (2009), which also pointed out that the water vapor feedback contributes significantly to the polar amplification. The finding, that the polar amplification is a strong interaction of many feedbacks and depending on the response in many regions globally, may explain to some degree why the uncertainty in the climate sensitivity is largest in the arctic regions in the IPCC-models ensemble. However, it needs to be noted that the arctic is a relative small and complex region. It is therefore likely that the results of the GREB model may have only limited relevance and some important feedbacks, such as atmospheric circulation and heat transport changes, are not simulated in the GREB model. It may however, in cooperation with CGCM models and observation, be a basis for a better understanding of the polar amplification.

Acknowledgments We like to thank two anonymous referees for their very helpful comments, which lead to a substantial improvement of the GREB model and the subsequent discussion. We also like to thank Mojib Latif for fruitful discussions and comments. Thorsten Simon helped in the numerical realization of the advection code and Tilman Rickert helped to improve some parameters of the GREB model.

Appendix 1

See Tables 1, 2 and 3.

Appendix 2

The 10 parameters, $pe_{1\text{-}10}$, of the emissivity model (Eqs. 4 and 5) can be constrained by literature values about the relationship between ε_{atmos} and the CO_2, $viwv_{atmos}$, and *CLD, and* some simple global constrains on the function. The following constraints, in order of importance, are considered for the model parameter fit:

1. The global mean $\varepsilon_{atmos} \approx 0.80 \pm 0.03$. The values follows from the slab greenhouse model for a given incoming global mean solar radiation, albedo and T_{surf} (Bohren and Clothiaux 2006). Regional differences, non-linearities and limitations of the model are estimated to give some uncertainty of about ± 0.03.
2. The IPCC estimated global change in thermal downward radiation of about 3.80 ± 0.33 W/m2 for doubling of CO_2 (Table 10.2 in Meehl et al. 2007a,

b) is in our model equivalent to $\Delta\varepsilon_{atmos}$ $(2 \times CO_2) \approx 0.019 \pm 0.003$. Uncertainties also include an estimate of regional differences, non-linearities and limitations of the model.

3. The effect of increased $viwv_{atmos}$ can be estimated in an inverse approach: Global mean changes in T_{surf} for doubling of CO_2 in the slab greenhouse model is about 1.1 K, while IPCC predications including all feedbacks lead to about 2.6. The ice-albedo feedback leads to about 20% increase of the warming in global average (Hall 2004). Assuming the remaining feedbacks are dominated by increased $viwv_{atmos,}$ we can estimate the $\Delta\varepsilon_{atmos}$ $(\Delta viwv_{atmos})$ to be about as strong as the $\Delta\varepsilon_{atmos}$ $(2 \times CO_2)$. Thus $\Delta\varepsilon_{atmos}$ $(\Delta viwv_{atmos}) \approx 0.02 \pm 0.003$. The $\Delta viwv_{atmos}$ can be approximated by assuming no changes in relative humidity, which corresponds to about 15% increase in absolute humidity for the IPCC predicted global mean T_{surf} changes.
4. The largest part of ε_{atmos} is due to $viwv_{atmos}$ (Mitchell 1989; Kiehl and Trenberth 1997). About 60% can be attributed to $viwv_{atmos}$, which in our model corresponds to $\Delta\varepsilon_{atmos}$ $(viwv_{atmos} \to 0) \approx 0.5 \pm 0.05$.
5. The emissivity of $viwv_{atmos}$ is mostly (¾) in the non-CO_2 overlapping spectral bands (see Fig. 6.2 in Peixoto and Oort 1992a, 1992b). This can be quantified in our model by:

$$\frac{a/3 - b}{(a/3 + b)/2} = 0 \pm 0.3$$
$$\text{with } a = pe_6 \cdot \log[pe_2 \cdot viwv_{atmos} + pe_3]$$
$$\text{and } b = pe_4 \cdot \log[pe_1 \cdot 340ppm + pe_2 \cdot viwv_{atmos} + pe_3] \quad (21)$$

6. The cloud effect on the surface thermal radiation is about 31 W/m^2 (Ramanathan et al. 1989). This converts in our model to $\Delta\varepsilon_{atmos}(CLD \to 0) \approx 0.16 \pm 0.05$.
7. The spectral emission of CO_2 and $viwv_{atmos}$ have bands which overlap (Peixoto and Oort 1992a, 1992b). In these bands (1. term RHS of Eq. 4) the relative contributions of CO_2 and $viwv_{atmos}$ should be about equal. This can be quantified in our model by:

$$\frac{a - b}{(a + b)/2} = 0 \pm 0.2 \text{ with } a = pe_1 \cdot 340\,\text{ppm} \quad \text{and}$$
$$b = pe_2 \cdot viwv_{atmos} \quad (22)$$

8. Cloud cover will increase the effective emissivity mostly by decreasing the sensitivity to trace gasses and lifting the effective emissivity mostly in regions with lower greenhouse gas concentraions (low $viwv_{atmos}$). While a literature discussion of this effect could not be found, the analysis of the ECHAM AGCM downward surface thermal radiation as a function of $viwv_{atmos}$ and CLD suggest that the sensitivity of ε_{atmos} to changes in $viwv_{atmos}$ is about twice as strong for clear sky than for cloudy conditions. This can be quantified in our model by:

$$\frac{a/2 - b}{(a/2 + b)/2} = 0 \pm 0.3$$
$$\text{with } a = \Delta\varepsilon_{atmos}(2xCO_2, \Delta viwv_{atmos}, CLD = 0)$$
$$\text{and } b = \Delta\varepsilon_{atmos}(2xCO_2, \Delta viwv_{atmos}, CLD = 1) \quad (23)$$

9. The CO_2 contributes to the emissivity by $\Delta\varepsilon_{atmos}(CO_2 \to 0) \approx 0.18 \pm 0.02$ (Ellingson and Fouquart 1991).
10. CO_2 spectral emission bands overlapping and non-overlapping with $viwv_{atmos}$ are about equally strong. (se Fig. 6.2 in Peixoto and Oort 1992a, 1992b). This can be quantified in our model by:

$$\frac{a - b}{(a + b)/2} = 0 \pm 0.5$$
$$\text{with } a = pe_5 \cdot \log[pe_1 \cdot 340ppm + pe_3]$$
$$\text{and } b = pe_4 \cdot \log[pe_1 \cdot 340ppm + pe_2 \cdot viwv_{atmos} + pe_3] \quad (24)$$

11. In absence of CO_2, $viwv_{atmos}$, and CLD the model should roughly be $\varepsilon_{atmos} \approx 0 \pm 0.3$.
12. In present climate a very humid atmosphere ($viw_{vatmos} = 70$ kg/m2) with complete cloud cover ($CLD = 1.0$) should represent the maximum $\varepsilon_{atmos} \approx 1.0 \pm 0.3$
13. The parameters $pe_{1–10}$ are positive definite.

The 13 constraints are used to set up a cost-function, in which each term is estimated under current climate conditions of CO_2, $viwv_{atmos}$, and CLD, globally averaged and normalized by the uncertainty, defining 12 error terms. The sum of the squared error terms is minimized by a numerical iterative scheme varying the parameters $pe_{1–10}$. The resulting parameters are listed in Table 2. The assumed global mean emissivity characteristics and the models estimated values under current climate conditions are listed in Table 4. Note, negative ε_{atmos} are only reached for $viwv_{atmos} < 1$ kg/m^2 and $CO_2 < 2$ ppm, which is faraway from the conditions to which the model is applied.

References

Alexeev VA, Langen PL, Bates JR (2005) Polar amplification of surface warming on an aquaplanet in "ghost forcing" experiments without sea ice feedbacks. Clim Dyn 24:655–666

Arrhenius S (1896) On the influence of carbonic acid on the air temperature of the ground. Philos Mag S5:237–276

Banks HT, Gregory JM (2006) Mechanisms of ocean heat uptake in a coupled climate model and the implications for tracer based predictions of ocean heat uptake. Geophys Res Lett 33(7):L07608

Barsugli JJ, Battisti DS (1998) The basic effects of atmosphere-ocean thermal coupling on midlatitude variability. J Atmospheric Sci 55:477–493

Bates JR (2007) Some considerations of the concept of climate feedback. Q J Royal Meteorol Soc 133:545–560

Bohren CF, Clothiaux EE (2006) Emissivity and global warming. Fundamentals of atmospheric radiation. Wiley, New Jersey, pp 31–41

Budyko MI (1969) The effect of solar radiation variation on the climate of the earth. Tellus 21:611–619

Budyko MI (1972) Future climate. Trans Am Geophys Union 53:868–874

Cai M (2006) Dynamical greenhouse-plus feedback and polar warming amplification. Part I: a dry radiative-transportive climate model. Clim Dyn 26:661–675

Cai M, Lu JH (2009) A new framework for isolating individual feedback processes in coupled general circulation climate models. Part II: method demonstrations and comparisons. Clim Dyn 32:887–900

Cess RD, Potter GL, Blanchet JP, Boer GJ, Delgenio AD, Deque M, Dymnikov V, Galin V, Gates WL, Ghan SJ, Kiehl JT, Lacis AA, Letreut H, Li ZX, Liang XZ, Mcavaney BJ, Meleshko VP, Mitchell JFB, Morcrette JJ, Randall DA, Rikus L, Roeckner E, Royer JF, Schlese U, Sheinin DA, Slingo A, Sokolov AP, Taylor KE, Washington WM, Wetherald RT, Yagai I, Zhang MH (1990) Intercomparison and interpretation of climate feedback processes in 19 atmospheric general-circulation models. J Geophys Res Atmospheres 95:16601–16615

Compo GP, Sardeshmukh PD (2009) Oceanic influences on recent continental warming. Clim Dyn 32:333–342

Curry JA, Schramm JL, Serreze MC (1995) Water-vapor feedback over the arctic-ocean. J Geophys Res Atmospheres 100:14223–14229

Dommenget D (2009) The ocean's role in continental climate variability and change. J Clim 22:4939–4952

Dommenget D, Latif M (2008) Generation of hyper climate modes. Geophys Res Lett 35(2):L02706

Ellingson RG, Fouquart Y (1991) The intercomparison of radiation codes in climate models—an overview. J Geophys Res Atmospheres 96:8925–8927

Fanning AF, Weaver AJ (1996) An atmospheric energy-moisture balance model: climatology, interpentadal climate change, and coupling to an ocean general circulation model. J Geophys Res Atmospheres 101:15111–15128

Ganopolski A, Petoukhov V, Rahmstorf S, Brovkin V, Claussen M, Eliseev A, Kubatzki C (2001) CLIMBER-2: a climate system model of intermediate complexity. Part II: model sensitivity. Clim Dyn 17:735–751

Graversen RG, Wang M (2009) Polar amplification in a coupled climate model with locked albedo. Clim Dyn 33:629–643

Hall A (2004) The role of surface albedo feedback in climate. J Clim 17:1550–1568

Harvey LDD, Schneider SH (1985) Transient climate response to external forcing on 10(0)–10(4) year time scales.1. Experiments with globally averaged, coupled, atmosphere and ocean energy-balance models. J Geophys Res Atmospheres 90:2191–2205

Held IM, Soden BJ (2000) Water vapor feedback and global warming. Ann Rev Energy Environ 25:441–475

James IN (1994) Introduction to circulating atmospheres. Cambridge University Press, Cambridge

Joshi MM, Gregory JM, Webb MJ, Sexton DMH, Johns TC (2008) Mechanisms for the land/sea warming contrast exhibited by simulations of climate change. Clim Dyn 30:455–465

Kalnay E, Kanamitsu M, Kistler R, Collins W, Deaven D, Gandin L, Iredell M, Saha S, White G, Woollen J, Zhu Y, Chelliah M, Ebisuzaki W, Higgins W, Janowiak J, Mo KC, Ropelewski C, Wang J, Leetmaa A, Reynolds R, Jenne R, Joseph D (1996) The NCEP/NCAR 40-year reanalysis project. Bull Am Meteorol Soc 77:437–471

Kiehl JT, Ramanathan V (1982) Radiative heating due to increased Co_2—the role of H2o continuum absorption in the 12–18 Mu-M region. J Atmospheric Sci 39:2923–2926

Kiehl JT, Trenberth KE (1997) Earth's annual global mean energy budget. Bull Am Meteorol Soc 78:197–208

Lambert FH, Chiang JCH (2007) Control of land-ocean temperature contrast by ocean heat uptake. Geophys Res Lett 34(13):L13704

Langen PL, Alexeev VA (2007) Polar amplification as a preferred response in an idealized aquaplanet GCM. Clim Dyn 29:305–317

Lorbacher K, Dommenget D, Niiler PP, Kohl A (2006) Ocean mixed layer depth: A subsurface proxy of ocean-atmosphere variability. J Geophys Res Oceans 111:C07010

Lu JH, Cai M (2010) Quantifying contributions to polar warming amplification in an idealized coupled general circulation model. Clim Dyn 34:669–687

Manabe S, Stouffer RJ (1980) Sensitivity of a global climate model to an increase of Co_2 concentration in the atmosphere. J Geophys Res Oceans Atmospheres 85:5529–5554

Manabe S, Stouffer RJ, Spelman MJ, Bryan K (1991) Transient responses of a coupled ocean atmosphere model to gradual changes of atmospheric Co_2.1. Annual mean response. J Clim 4:785–818

Meehl GA, Covey C, Delworth T, Latif M, McAvaney B, Mitchell JFB, Stouffer RJ, Taylor KE (2007) The WCRP CMIP3 multimodel dataset—a new era in climate change research. Bull Am Meteorol Soc 88:1383

Meehl GA, Stocker TF, Collins WD, Friedlingstein P, Gaye AT, Gregory JM, Kitoh A, Knutti R, Murphy JM, Noda A, Raper SCB, Watterson IG, Weaver AJ, Zhao Z-C (eds) (2007b) Global climate projections. Climate change 2007: the physical science basis. Contribution of working group I to the fourth assessment report of the intergovernmental panel on climate change. Cambridge University Press, Cambridge

Mitchell JFB (1989) The greenhouse-effect and climate change. Rev Geophys 27:115–139

Murphy JM, Sexton DMH, Barnett DN, Jones GS, Webb MJ, Collins M (2004) Quantification of modelling uncertainties in a large ensemble of climate change simulations. Nature 430:768–772

Myhre G, Highwood EJ, Shine KP, Stordal F (1998) New estimates of radiative forcing due to well mixed greenhouse gases. Geophys Res Lett 25:2715–2718

North GR, Cahalan RF, Coakley JA (1981) Energy-balance climate models. Rev Geophys 19:91–121

Peixoto JP, Oort AH (1992) Radiation balance. Phys Clim Springer:91–130

Peixoto JP, Oort AH (1992b) Physics of climate. Springer, New York, p 520

Petoukhov V, Claussen M, Berger A, Crucifix M, Eby M, Eliseev AV, Fichefet T, Ganopolski A, Goosse H, Kamenkovich I, Mokhov II, Montoya M, Mysak LA, Sokolov A, Stone P, Wang Z, Weaver AJ (2005) EMIC Intercomparison Project (EMIP-CO_2): comparative analysis of EMIC simulations of climate, and of equilibrium and transient responses to atmospheric CO_2 doubling. Clim Dyn 25:363–385

Pierrehumbert RT (1995) Thermostats, radiator fins, and the local runaway greenhouse. J Atmospheric Sci 52:1784–1806

Ramanathan V (1977) Interactions between ice-albedo, lapse-rate and cloud-top feedbacks—analysis of non-linear response of a GCM climate model. J Atmospheric Sci 34:1885–1897

Ramanathan V, Lian MS, Cess RD (1979) Increased atmospheric Co_2—zonal and seasonal estimates of the effect on the radiation energy-balance and surface-temperature. J Geophys Res Oceans Atmospheres 84:4949–4958

Ramanathan V, Cess RD, Harrison EF, Minnis P, Barkstrom BR, Ahmad E, Hartmann D (1989) Cloud-radiative forcing and climate—results from the earth radiation budget experiment. Science 243:57–63

Rapti AS (2005) Spectral optical atmospheric thickness dependence on the specific humidity in the presence of continental and maritime air masses. Atmospheric Res 78:13–32

Roeckner EG, Bäuml L, Bonaventura R, Brokopf M, Esch M, Giorgetta S, Hagemann I, Kirchner L, Kornblueh E, Manzini A, Rhodin SU, Schulzweida U, Tompkins A (2003) The atmospheric general circulation model ECHAM 5. Part I: model description. Rep Max Planck Inst Meteorol 349

Rossow WB, Schiffer RA (1991) Isccp cloud data products. Bull Am Meteorol Soc 72:2–20

Sellers WD (1965) Physical climatology. University of Chicago Press, Chicago, p 272

Sellers WD (1969) A climatic model based on the energy balance of the earth-atmosphere system. J Appl Meteorol 8:392–400

Sellers WD (1976) 2-dimensional global climatic model. Mon Weather Rev 104:233–248

Serreze MC, Francis JA (2006) The arctic amplification debate. Climat Chang 76:241–264

Soden BJ, Held IM (2006) An assessment of climate feedbacks in coupled ocean-atmosphere models. J Clim 19:3354–3360

Sutton RT, Dong BW, Gregory JM (2007) Land/sea warming ratio in response to climate change: IPCC AR4 model results and comparison with observations. Geophys Res Lett 34(2):L02701

Weaver AJ, Eby M, Wiebe EC, Bitz CM, Duffy PB, Ewen TL, Fanning AF, Holland MM, MacFadyen A, Matthews HD, Meissner KJ, Saenko O, Schmittner A, Wang HX, Yoshimori M (2001) The UVic earth system climate model: model description, climatology, and applications to past, present and future climates. Atmosphere Ocean 39:361–428

Webb MJ, Senior CA, Sexton DMH, Ingram WJ, Williams KD, Ringer MA, McAvaney BJ, Colman R, Soden BJ, Gudgel R, Knutson T, Emori S, Ogura T, Tsushima Y, Andronova N, Li B, Musat I, Bony S, Taylor KE (2006) On the contribution of local feedback mechanisms to the range of climate sensitivity in two GCM ensembles. Clim Dyn 27:17–38

Winton M (2006) Amplified Arctic climate change: what does surface albedo feedback have to do with it? Geophys Res Lett 33(3):L03701

Zhang R, Delworth TL, Held IM (2007) Can the Atlantic ocean drive the observed multidecadal variability in Northern Hemisphere mean temperature? Geophys Res Lett 34(2):L02709